

Spectroscopic investigations, DFT calculations, molecular docking and MD simulations of 3-[(4-Carboxyphenyl) carbamoyl]-4-hydroxy-2-oxo-1, 2-dihydroxy quinoline-6-carboxylic acid.

P. K. Ranjith^{a,b}, Angel Ignatious^c, C. Yohannan Panicker^d, B. Sureshkumar^e, Stevan Armakovic^f, Sanja J. Armakovic^g, C. Van Alsenoy^h, P. L. Anto^{a,c*}

^a Department of Physics, Christ College (Autonomous), Irinjalakuda, Thrissur, Kerala, India

^b Department of Physics, MPMMSN Trusts College, Shoranur, Palakkad, Kerala, India

^c Department of Physics, St. Joseph's College (Autonomous), Irinjalakuda, Thrissur, Kerala, India

^d Thushara, Neethinagar-64, Kollam, Kerala, India.

^e Department of Chemistry, Sree Narayana College, Kollam, Kerala, India

^f University of Novi Sad, Faculty of Sciences, Department of Physics, Trg D. Obradovica 4, 21000 Novi Sad, Serbia

^g University of Novi Sad, Faculty of Sciences, Department of Chemistry, Biochemistry and Environmental Protection, Trg D. Obradovica 3, 21000 Novi Sad, Serbia

^h Department of Chemistry, University of Antwerp, Groenenborgerlaan 171, B-2020, Antwerp, Belgium

* Corresponding author: email address: antoponnore367@gmail.com (P. L. Anto)

Abstract

By FT-IR, FT-Raman and DFT computations spectral characterisation of 3-[(4-Carboxyphenyl) carbamoyl]-4-hydroxy-2-oxo-1, 2-dihydroxy quinoline-6-carboxylic acid was performed. Computational calculations were done using B3LYP/6-31G(d') basis set. Vibrational assignments of wavenumbers were performed on the basis of potential energy distribution. Donor acceptor interactions were evaluated using NBO analysis. To foresee the important reactive sites of the title compound we combined DFT calculations and molecular dynamics (MD) and

visualized the ALIE and Fukui functions. Sensitive nature of the compound towards autoxidation and degradation in the presence of water was investigated by the calculation of BDE and RDF. By molecular docking the compound forms a stable complex with ubiquinol-cytochrome-c reductase inhibitor.

Keywords: Quinoline, DFT, ALIE, RDF, BDE, Solubility, Molecular Docking

1. Introduction

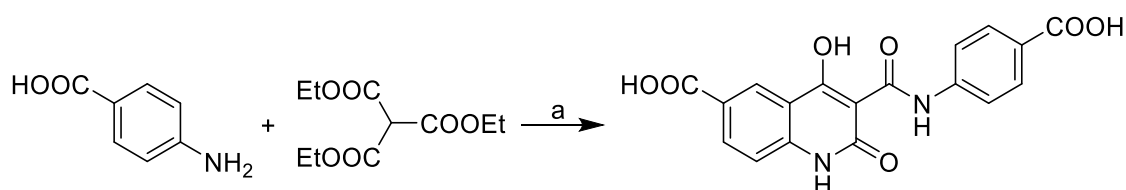
Quinoline derivatives possess number of medicinal properties like anti-bacterial [1] anti-filarial [2] anti-malarial [3] anti-fungal [4] cardiovascular [5] anti-tuberculosis [6]. 8-hydroxy quinoline derivative can be used as an active compound of pharmaceutical products [7] nuclear medicine [8] treating cancer [9] and neurodegeneration disorder [10]. Recent years DFT, molecular docking and vibrational studies of quinoline derivatives are reported [11,12]. Some quinoline derivatives are used as lifesaving drugs and have many applications like optical switches sensors in electro chemistry and in the area of inorganic chemistry [13,14]. Amino quinoline derivatives are a good candidate for the inhibition of human immuno virus (HIV) [15]. In order to analyse the effect of halogen substitution, in the parent molecule the hydrogen atoms 7H, 8H and 9H are replaced by fluorine, chlorine and bromine atoms which are designated as 7F, 8F, 9F for fluorine, 7Cl, 8Cl, 9Cl for chlorine and 7Br, 8Br, 9Br for bromine, respectively. Here we have spectroscopically characterized the title compound by employing FT-IR and FT-Raman techniques and to predict the local as well as global reactive properties by DFT calculations and MD simulations. Using DFT calculations we have also calculated the Frontier molecular orbitals (FMO) which helps us in understanding the HOMO-LUMO gap which determines the stability, hardness and many other parameters. To foresee about the reactive sites ALIE, MEP and Fukui function values are plotted against to the electron density surface. Thus, we can evaluate the prone sites of electrophilic and nucleophilic attacks. Organic molecules with considerable biological activity and high stability are usually a threat to the nature [16]. Autoxidation and hydrolysis are important parameters that helps to analyse the degradation properties of the molecule. BDE (Bond dissociation energy) and RDF (Radial distribution functions) reflect the sensitivity of compounds towards the water environments, BDE and RDF can be evaluated using the MD simulations and DFT calculations. The greatest challenge in the production of pharmaceutical products is to find an active component, if the active component doesn't meet the

requirements, it can be modified using an excipient. Using solubility parameter, we can easily find out an excipient [17-19]. Therefore, the aim of our study was to calculate and understand the degradation properties of target molecule, to check a suitable excipient and to perform molecular docking.

2. Experimental Details

3-[(4-Carboxyphenyl)carbamoyl]-4-hydroxy-2-oxo-1,2-dihydroquinoline-6-carboxylic acid was prepared by a microwave-assisted reaction of 4-aminobenzoic acid with triethyl methanetricarboxylate [20] (Scheme 1). All reagents were purchased from Aldrich. Kieselgel 60, 0.040-0.063 mm (Merck, Darmstadt, Germany) was used for column chromatography. TLC experiments were performed on alumina-backed silica gel 40 F254 plates (Merck). The plates were illuminated under UV (254 nm) and evaluated in iodine vapour. The melting points were determined on Boetius PHMK 05 (VEB Kombinat Nagma, Radebeul, Germany) and are uncorrected. Elemental analyses were carried out on an automatic Perkin-Elmer 240 microanalyser (Boston, USA). The purity of the final compounds was checked by the HPLC separation module Waters Alliance 2695 XE (Waters Corp., Milford, MA, USA). The detection wavelength 210 nm was chosen. The peaks in the chromatogram of the solvent (blank) were deducted from the peaks in the chromatogram of the sample solution. The purity of individual compounds was determined from the area peaks in the chromatogram of the sample solution. UV spectra (λ , nm) were determined on a Waters Photodiode Array Detector 2996 (Waters Corp.) in ca 6×10^{-4} mol methanolic solution and $\log \epsilon$ (the logarithm of molar absorption coefficient ϵ) was calculated for the absolute maximum λ_{\max} of individual target compounds. All ^1H NMR spectra were recorded on a Bruker AM-500 (499.95 MHz for ^1H), Bruker Bio Spin Corp., Germany. Chemical shifts are reported in ppm (δ) to internal $\text{Si}(\text{CH}_3)_4$, when diffused easily exchangeable signals are omitted.

2.1 3-[(4-Carboxyphenyl) carbamoyl]-4-hydroxy-2-oxo-1, 2-dihydroxy quinoline-6-carboxylic acid.



Scheme 1. Preparation of the target compound: (a) microwave irradiation

4-Aminobenzoic acid (0.7 g, 0.005 mol) was mixed with triethyl methanetricarboxylate (2.12 mL, 0.01 mol) and heated in microwave reactor at 50% of power during 15 min and 3 min at 90%. The temperature reached 231 °C during heating. Et₂O was added to the cooled mixture and the precipitate was washed with hot (55 °C) MeOH to obtain the pure product as a yellow crystalline compound. Yield 62%. Mp 340-350 °C. Anal. Calc. for C₁₈H₁₂N₂O₇ (368.29): C 58.70%, H 3.28%; found: C 58.09%, H 3.54%. HPLC purity 97.52%. UV (nm), λ_{max}/log ε: 251.3/3.53. IR (cm⁻¹): 3621, 1180 (OH), 3034 (CH_{arom}), 2970, 1689 (acid), 1680 (lactam), 1642 (C=O), 1635 (C = C_{cycle}), 1630 (amide), 1599 (Ph), 1520 (NH). ¹H NMR (DMSO-*d*₆, 500 MHz) δ: 7.41 (d, *J*=8.5 Hz, 1H), 7.70 (d, *J*=9.1 Hz, 2H), 7.90 (d, *J*=9.1 Hz, 2H), 8.15 (d, *J*=8.5 Hz, 1H), 8.50 (s, 1H), 12.40 (s, 1H), 12.95 (s, 1H), 16 (s, 1H).

The FT-IR spectrum (Fig.1) was recorded using KBr pellets on a DR/Jasco FT-IR 6300 spectrometer. The FT-Raman spectrum (Fig.2) was obtained on a Bruker RFS 100/s, Germany. For excitation of the spectrum the emission of Nd: YAG laser was used, excitation wavelength 1064 nm, maximal power 150mW, measurement on solid sample.

3. Computational Details

Calculations of the wavenumbers, molecular geometry, polarizability values, frontier molecular orbital analysis were carried out with Gaussian 09 program [21] using the B3LYP/6-31G(d') quantum chemical calculation method. A scaling factor of 0.9613 is used to scale the theoretically obtained wavenumbers [22] and the assignments of the vibrational wavenumbers are done by using Gauss View [23] and GAR2PED software [24]. Parameters corresponding to optimized geometry of the title compound (Fig. 3) are given in Table 1. Jaguar 9.0 and Schrodinger materials science suite 2015-4 was used for the investigation of the reactivity of the compound [25]. DFT calculations with the Jaguar were carried out using B3LYP exchange correlation functional, with 6-311++G(d,p), 6-31+G(d,p) and 6-311G(d,p) basis sets for the calculations of ALIE, Fukui functions and BDEs, respectively. Desmond program was used for MD simulations which was performed by OPLS 2005 force field [26], with simulation time set to 10 ns. The pressure was set at 1.0325 bar while temperature was set to 300 K. Cutoff radius was set to 12 Å, while the modelled system was of isothermal-isobaric (NPT) ensemble class. For the solvent of SPC model [27] was used here. For the modelling of system CPCHODQ6C

molecule was placed alone into the cubic box with ~3000 water molecules. For the preparation of input files and output analysis Schrodinger materials science suite 2015-4 was used [28].

4. Results and Discussions

4.1 Optimized Geometrical Parameters

For the title compound the bond lengths of C₂-C₃ = 1.4084 Å, C₃-C₄ = 1.4130 Å and C₄-C₅ = 1.4045 Å and these values are greater than that of C₁-C₂ (1.3824 Å) and C₅-C₆ (1.3916 Å) due to adjacent quinoline ring and the reported values are C₂-C₃ = 1.4020 Å, C₃-C₄ = 1.4171 Å, C₅-C₄ = 1.4043 Å [29]. The values of bond lengths C₁₂-C₁₄ (1.4579 Å) and C₁₄-C₁₈ (1.4854 Å) are high which is due to the adjacent C=O and carboxylic groups. The bond angle C₃-C₄-C₅ (119.5°) is lesser than 120° because of the presence of quinoline ring. The angles C₄-C₁₃-C₁₄ and C₃-N₁₀-C₁₂ are 121.2° and 126.0° respectively, which can be assumed as due to the presence of OH group which is electropositive. According to literature the corresponding reported bond angles are C₁-C₂-C₃ (119.6°), C₂-C₃-C₄ (119.4°), C₂-N₁₄-C₂₀ (125.8°), C₃-C₁₅-C₁₈ (121.3°) and N₁₄-C₂₀-C₁₈ (114.2°) respectively [30]. The presence of higher electro negative group C=O would be the reason for the lesser bond angle of N₁₀-C₁₂-C₁₄ (116.0°).

4.2 IR and Raman Spectra

The observed IR and Raman bands and calculated (scaled) wavenumbers and assignments are given in Table 2. The C₁₂=O₁₆ and C₁₃=C₁₄ stretching vibrations are assigned at 1678 cm⁻¹ (DFT), 1670 cm⁻¹ (IR) and at 1562 cm⁻¹ (DFT), 1551 cm⁻¹ (IR), 1548 cm⁻¹ (Raman) respectively. The C=O stretching mode has high IR intensity and PED of 37%. The C=O stretching vibration in the spectra of carboxylic acid give rise to strong bands in the region 1600-1700 cm⁻¹ [31]. The bands observed at 1746, 1741 cm⁻¹ theoretically with IR intensities 362.66, 401.29, Raman activities 269.81, 169.61 and with PEDs of 73, 72% are assigned as C₃₅=O₃₆, C₃₁=C₃₂ stretching modes of the title compound. The stretching band of C₁₃-O₁₅ is expected in the region 1220 ± 40 cm⁻¹ [32-34] and the band at 1292 cm⁻¹ (DFT) is assigned as C-O stretching vibration with IR intensity of 165.43, Raman activity of 5.51 and a PED of 17% of the title compound while the reported value is 1206 cm⁻¹(DFT) [30]. The O-H stretching vibration gives rise to a band at 3050 ± 150 cm⁻¹ [31]. The band observed at 2666

cm^{-1} experimentally and 2793 cm^{-1} in DFT calculation is assigned as the O-H stretching vibration. The downshift of the OH stretching mode is due to the strong hydrogen bonded system present in the title compound as reported in literature [35, 36]. The O-H in-plane and out-of-plane deformation modes are expected at $1395 \pm 55 \text{ cm}^{-1}$ and at $905 \pm 70 \text{ cm}^{-1}$ respectively [32]. For the title compound the band at 1352 cm^{-1} (DFT) is assigned as the in-plane O-H deformation band. Similarly, the band at 922 cm^{-1} (DFT) is assigned as the O-H out-of-plane deformation band of the title compound. The in-plane O-H bending mode has a low IR intensity 68.74 and high Raman activity of 955.36. Rajeev et al. [30] reported a band at 1412 cm^{-1} as the in-plane O-H deformation. The N-H stretching vibrations are expected [37] in the range $3500\text{-}3300 \text{ cm}^{-1}$. In the present study the bands observed at $3440, 3392 \text{ cm}^{-1}$ in the IR spectrum and 3454 cm^{-1} theoretically are assigned as N-H stretching vibrational mode which has a PED of 100%, IR intensity 50.89 and Raman activity 108.89. In the present case the N-H stretching mode splits into a doublet and downshifted from the computed value which indicates the weakening of the N-H bond [38, 39]. N-H group shows bands at $1510\text{-}1500, 1350\text{-}1250$ and $740\text{-}730 \text{ cm}^{-1}$ [39]. According to literature if N-H is a part of a closed ring [40] the N-H deformation band is absent in the region $1510\text{-}1500 \text{ cm}^{-1}$. In the present case the N-H in-plane deformation band is observed at 1439 cm^{-1} theoretically and this mode has IR intensity 35.79, Raman activity 131.12 with a PED 22%. The out-of-plane deformation bands of N-H are expected in the range $650 \pm 50 \text{ cm}^{-1}$ and the bands observed at 612 cm^{-1} (DFT) are assigned as $\gamma\text{N-H}$ mode of the title compound. This mode has 73% PED with 60.95 as IR intensity and a low Raman activity less than 10.00. In the present case, the quinoline CC stretching ring modes are observed at 1413 cm^{-1} in the IR spectrum, 1414 cm^{-1} in the Raman spectrum, 1413 cm^{-1} theoretically with high Raman activity and the C-N stretching modes are at 1114 cm^{-1} in the IR spectrum, $1233, 1106, 1082 \text{ cm}^{-1}$ theoretically. Both the modes possess moderate IR intensities. Rajeev et al. reported the quinoline stretching modes at $1610, 1445, 1020 \text{ cm}^{-1}$ (C-C), 1262 cm^{-1} (C-N) in the IR spectrum, $1609, 1051, 1022 \text{ cm}^{-1}$ (C-C), 1202 cm^{-1} (C-N) in the Raman spectrum, $1607, 1433, 1045, 1035 \text{ cm}^{-1}$ (C-C), $1270, 1230 \text{ cm}^{-1}$ (C-N) theoretically [30]. The DFT calculations give the C-H stretching modes of the phenyl ringI and phenyl ringII of the title compound at $3128, 3101, 3067 \text{ cm}^{-1}$ and $3151, 3099, 3098, 3061 \text{ cm}^{-1}$. Similarly, the bands observed at $3132, 3103, 3078 \text{ cm}^{-1}$ (Raman) and $3157, 2990 \text{ cm}^{-1}$ (IR) are assigned as C-HI and C-HII stretching modes of the phenyl rings of parent molecule [31]. The bands observed at $1470, 1372$ and $1593, 1505, 1314 \text{ cm}^{-1}$ in IR spectrum, 1477 and $1602, 1503, 1382, 1323 \text{ cm}^{-1}$ in Raman spectrum and at $1618, 1580, 1485, 1369, 1342$ and $1609, 1591,$

1538,1403,1321 cm^{-1} theoretically are assigned as phenyl rings stretching modes of the title compound which are expected in the region 1620-1250 cm^{-1} [31]. In asymmetric tri-substituted benzene, when all the three substituents are heavy, the ring breathing mode appears above 1100 cm^{-1} [32]. For the tri-substituted phenyl ring PhI, the ring breathing mode is assigned at 1066 cm^{-1} theoretically with moderate IR intensity and PED 18%. Madhavan et al. [41] reported the ring breathing mode for a compound having two tri-substituted benzene rings at 1110 and 1083 cm^{-1} respectively. In the present case, the band observed at 1070 cm^{-1} in Raman spectrum and 1072 cm^{-1} theoretically with a PED contribution of 36% and high IR intensity is assigned as the ring breathing mode of the phenyl ring II which is expected in region 1020-1070 cm^{-1} [32]. Panicker et al. [42] reported the ring breathing mode of di-substituted benzene at 1018 cm^{-1} (IR), 1034 cm^{-1} (Raman) and 1019 cm^{-1} (DFT). For the title compound, the bands observed at 1284 cm^{-1} (IR), 1134, 1099, cm^{-1} (Raman) and 1288, 1245, 1152, 1137, 1104 cm^{-1} (DFT) are assigned as the C-H in-plane bending modes of the phenyl rings. The C-H out-of-plane deformations are expected below 1000 cm^{-1} [31] and for the title compound the theoretical calculations give bands at 951, 949, 938, 925, 842, 828, 815, 794 cm^{-1} as γ C-H modes of the phenyl rings. Experimentally these bands are observed at 970, 926, 841, 818, 799 cm^{-1} in the Raman spectrum.

4.3 Frontier Molecular Orbitals

Frontier molecular orbital study is used to explain the chemical behaviour and stability of the molecular system. The atomic orbital components of the frontier molecular orbitals are shown in Fig. 4. The delocalization of HOMO and LUMO over the molecular system shows the charge transfer within the molecular system. The HOMO-LUMO gap is found to be 3.157 eV. The chemical descriptors can be evaluated by using HOMO and LUMO orbital energies, E_{HOMO} , and E_{LUMO} as ionization energy $I = -E_{\text{HOMO}}$, electron affinity $A = -E_{\text{LUMO}}$, hardness $\eta = (I-A)/2$, chemical potential $\mu = -(I+A)/2$ and electrophilicity index ($\omega = \mu^2/2\eta$) [43]. For the title compound CPCHODQ6C, $I = 8.482$, $A = 5.325$, $\eta = 1.579$, $\mu = -6.904$ and $\omega = 15.093$ eV (Table 3). For the title molecule, HOMO is delocalized over the phenyl group (PhII), amide group and partially over the quinoline ring while the LUMO is delocalized strongly over the entire molecule except carboxyl group of quinoline ring. For 7Cl, HOMO is delocalized strongly over the quinoline ring and substituted chlorine atom while LUMO is delocalized strongly over the entire molecule except NH groups. For 8Cl and 9Cl HOMO is

over the phenyl ring PhI and partially over the pyridine ring and LUMO is over the entire molecule except carboxyl group of PhI and carbonyl group of pyridine ring. For 7Br HOMO is over the entire molecule except carboxyl group of PhI and LUMO is over the entire molecule. For 8Br and 9Br HOMO is over the entire molecule except carboxyl group of PhI and carbonyl group of pyridine ring and LUMO is over the entire molecule except carboxyl group of PhI and NH group of pyridine ring. For 7F, HOMO is over the entire molecule except carboxyl group of PhI and NH of pyridine while LUMO is over the entire molecule except NH group of amide group. For 8F, HOMO is over the entire quinoline ring while for 9F, HOMO is over the entire molecule. LUMO is delocalized over the entire molecule except carboxyl group of PhI, carbonyl group of pyridine and NH group of amide for 8F and 9F. The chemical potential decreases for the halogen substitution in the order 7Cl, 8Cl, 9Cl < 7F, 8F, 9F < 7Br, 8Br, 9Br < CPCHODQ6C. Chemical potential value of 8Cl is deviated maximum from the parent molecule while all other halogen substitution shows minimum deviation. Halogen substitution results in reduction in the μ value in comparison with the parent molecule and for 8Cl it is minimum. Halogen substitution also results a decrease in electrophilicity index and is minimum for 8Cl. Global hardness is higher for 8Cl because of its large HOMO-LUMO gap which results a decrease in polarizability.

4.4 *Molecular Electrostatic Potential*

Molecular electrostatic potential and electron density are related to each other to find the reactive sites for electrophilic and nucleophilic sites [44,45]. The negative (red and yellow) regions of MEP map (Fig.5) were related to electrophilic reactivity while the positive (blue) regions to nucleophilic reactivity. For the parent molecule, most electrophilic (red and Yellow) regions are C=O group of both carboxyl group, slightly over PhII and the nucleophilic regions (blue) are deeply over the NH bond of quinoline ring, slightly over the hydrogen atom of the OH groups. For 7Cl, 8Cl and 9Cl, electrophilic regions are strongly over the carbonyl group of both carboxyl group and slightly over the phenyl ring while the nucleophilic regions are over the NH group of quinoline ring and slightly over the hydrogen atoms of the OH groups and more intense in the case of 8Cl. For fluorine substitution the electrophilic regions are similar to that of chlorine substitution while the nucleophilic regions are same that of chlorine substitution but blue region of NH bond of quinoline in 8F is more pronounced. For bromine substitution also the electrophilic and nucleophilic behaviour is identical to that of chlorine and fluorine substitution while blue region around bromine is

higher than that in fluorine substitution. The nucleophilic region of fluorine substitution is less than that in chlorine and bromine substitution.

4.5 NBO Analysis

The natural bond orbitals (NBO) calculations were performed using NBO 3.1 program [46] and the important interactions are presented in tables 4 and 5. The strong interactions are $LPO_{37} \rightarrow C_{35}-O_{36}$, $LPO_{36} \rightarrow C_{35}-O_{37}$, $LPO_{33} \rightarrow C_{31}-O_{32}$, $LPO_{32} \rightarrow C_{31}-O_{33}$, $LPN_{20} \rightarrow C_{18}-O_{19}$, $LPO_{15} \rightarrow C_{13}-C_{14}$, $LPN_{10} \rightarrow C_{12}-O_{16}$, $LPC_4 \rightarrow C_{13}-C_{14}$ and $LPC_4 \rightarrow C_5-C_6$ with energies, 21.44, 16.30, 21.43, 16.26, 28.99, 22.49, 27.67, 37.81 and 35.28 kcal/mol. 100% p-character is found in lone pairs of O_{37} , O_{36} , O_{33} , O_{32} , O_{16} , O_{15} and N_{10} atoms.

4.6 Nonlinear Optical Properties

The calculated first hyper polarizability of the title compound is 15.827×10^{-30} esu which is 121.75 times that of standard NLO material urea (0.13×10^{-30} esu) (Table 6) [47]. The reported value of first hyper polarizability of similar derivative is 2.24×10^{-30} esu [48]. The phenyl ring stretching vibrations at 1593, 1505 cm^{-1} in the IR spectrum have their counterparts in the Raman spectrum at 1602, 1503 cm^{-1} respectively with IR and Raman intensities are comparable. These types of organic molecules have conjugated π -electron system and large hyper polarizability which leads to nonlinear optical properties [49]. The C–N distances in the calculated molecular structure vary from 1.3745 to 1.4047 Å which are in between those of a CN single and double bond and this suggest an extended π -electron delocalization over the molecular system which is also responsible for the nonlinearity of the molecule [50]. We conclude that the title compound is an attractive object for future studies of non-linear optical properties.

4.7 ALIE surfaces and Fukui functions

Average local ionization energy (ALIE) is a quantum molecular descriptor which indicates the energy required to remove an electron from the molecule. So, we can say that the sites with least values of ALIE are more open for an electrophilic attack [51,52]. According to the equation given below ALIE is the sum of orbital energies weighted by the orbital density.

$$I(r) = \sum_i \frac{\rho_i(\vec{r}) \varepsilon_i}{\rho(\vec{r})}$$

Where $\rho_i(\vec{r})$ denotes electronic density of the i -th molecular orbital at the point \vec{r} , ε_i denotes orbital energy and $\rho(\vec{r})$ denotes total electronic density function. We have mapped the ALIE values with the electron density surface in order to understand the attacking sites of electrophiles. The ALIE figure is represented in Fig. 6. Here in this figure, we can see that benzene ring shows the least ALIE values that is 210.59 kcal/mol. On the other side in the close vicinity of hydrogen atoms H₁₁, H₁₇, H₃₄, H₃₈, H₃₉ shows highest ALIE value 372.51 kcal/mol. The interesting molecular sites which are important in the view of local reactivity can be identified using Fukui functions. The functional derivative of chemical potential with respect to external potential is termed as Fukui functions. According to Maxwell's relations we can interpret this as the derivative of electronic density with respect to the number of electrons [53-55]. If we physically interpret the term, it is the change in electron density according to change in charge. These functions in Jaguar program are calculated with the help of finite difference approach, according to the following equations:

$$f^+ = \frac{(\rho^{N+\delta}(r) - \rho^N(r))}{\delta},$$

$$f^- = \frac{(\rho^{N-\delta}(r) - \rho^N(r))}{\delta},$$

where N stands for the number of electrons in reference state of the molecule, while δ stands for the fraction of electron which default value is set to be 0.01[55]. By plotting Fukui functions to electron density surfaces we get a lot of information about the important molecular sites acting as a reactive centres [51,52]. The Fukui function plot is represented in Fig. 7. The colour coding in the plot is as follows, purple (positive) colour in Fukui function f^+ means the electron density has been increased by the addition of charges to the system while red (negative) colour in Fukui function f^- means the electron density has been diminished by the addition of charges. Electron density is increased in the near vicinity of carbon atom C₂₁ and electron density is decreased near the O₁₆, O₃₆, O₃₇ atoms.

4.8 *Reactive and degradation properties based on autoxidation and hydrolysis*

Degradation properties based on autoxidation and hydrolysis mechanisms are explained using RDFs and BDEs. Calculations of BDE for hydrogen abstraction allow the possibility to predict molecular sites where autoxidation process could start. It provides details about upto what extent some molecule are sensitive to presence of oxygen in open air, a parameter that is of very much importance in pharmaceutical industry. Forced degradation studies can also be studied using BDE, since they can be used for confirmation and determination of degradation path of some organic pharmaceutical molecule [56-59]. Wright et al. says that the target molecule is most vulnerable to autoxidation if the BDE for hydrogen abstraction ranges from 70 to 85 kcal/mol [60]. BDE values for hydrogen abstraction lower than 70 kcal/mol, are not suitable for the autoxidation mechanism since formed radicals are resistant for O₂ insertion [60-62]. Fig.8 contains all BDE values for CPCHODQ6C. Red coloured values represent the BDE values for hydrogen abstraction and blue-coloured values correspond to the BDE values for the rest of the single acyclic bonds. All the BDE values of molecule are greater than 100 kcal/mol so we can say that the molecule is stable in the presence of oxygen. To find the extend of hydrolysis we have also calculated the RDF for the molecule. In Fig.9 RDFs of atoms with the most pronounced interactions with water molecules are presented. In RDF plot, $g(r)$ represents the probability of finding a particle in the distance r from another particle [63]. Results provided in Fig.9 indicate that only four atoms of CPCHODQ6C molecule have relatively significant interactions with water molecules. These atoms are C₁₂, C₂₄, O₁₉, O₃₃, O₃₇, H₁₁, H₁₇, H₃₄, H₃₈, H₃₉ which shows similar $g(r)$ profile. According to the maximal $g(r)$ values the most important RDF is certainly for H₃₄ atom. Here the presence of hydrogen atoms shows the low stability of the molecule in the surroundings of water, so the role of this title compound in the pharmaceutical industry is irrelevant.

4.9 *Solubility parameter*

One of the demanding fields in pharmaceutical is the development of new products and finding the active component. To be considered for the pharmaceutical drug production, the active ingredient has to fit in to certain physical properties such as stability, solubility etc. If

the active component doesn't meet the required parameters, then these properties must be modified. One way to modify the properties without structural modification is to find a suitable excipient and mixing them up. Suitable excipient can be identified using experimental methods but its time consuming, while computational methods can be effectively used to narrow down the possibilities. Active component and excipient must be mutually compatible, one of the parameters for compatibility is the solubility parameter. Which means, the solubility parameter of the active component must have a value similar to the one of the excipient compounds [17-19]. Solubility parameter can be computationally predicted by applying the MD simulations and the following equation:

$$\delta = \sqrt{\frac{\Delta H_V - RT}{V_m}} \quad (1)$$

In this work, the solubility parameter has been calculated for the CPCHODQ6C molecule and it has been compared with three compounds frequently used as excipients polyvinylpyrrolidone polymer (PVP), maltose, and sorbitol). MD systems used to calculate this quantity consisted of 32 molecules placed in a cubic simulation box. Solubility parameters of all mentioned compounds have been summarized in Table 7.

As indicated by the results presented in Table 7, the CPCHODQ6C molecule has the highest compatibility with the Maltose compound. In this case, the difference between corresponding values of solubility parameter is less than $0.2 \text{ MPa}^{1/2}$, indicating very high compatibility. Solubility parameter of sorbitol is higher than the solubility parameter of the CPCHODQ6C molecule, while PVP has lesser value than our title molecule. Therefore, the MD calculations suggest that it is reasonable to consider Maltose as an excipient for CPCHODQ6C molecule.

4.10 Molecular Docking

Antimalarial drugs constitute a major part of antiprotozoal drugs. Malaria remains a major health problem, mainly in sub-Saharan Africa and parts of Asia and South America [64] with over 200 million clinical infections and nearly half a million deaths annually. Malaria is caused by protozoan parasites belonging to the genus Plasmodium and is transmitted via the bite of a female Anopheles mosquito. There are four major species of the parasite that cause malaria in humans, namely, Plasmodium falciparum, P. vivax, P. ovale and P. malaria, while a fifth parasite, P. knowlesi, is now recognized [65]. Historically, a range of drugs has been used to treat or prevent malaria, including several derived from the quinoline ring system

such as quinine, chloroquine (CQ), amodiaquine, piperaquine, mefloquine, and primaquine [66]. Quinoline and its related derivative comprise a class of heterocycles, which has been exploited immensely than any other nucleus for the development of potent antimalarial agents. Various chemical modifications of quinoline have been attempted to achieve analogs with potent antimalarial properties against sensitive as well as resistant strains of *Plasmodium* sp., together with minimal potential undesirable side effects [67]. From PASS (Prediction of Activity Spectra) [68] analysis we have to choose the favorable target for docking study and different types of activities predicted as in Table 8. We choose the activity ubiquinol-cytochrome-c reductase inhibitor with Pa value 0.858 and high-resolution crystal structure of corresponding receptor atovaquone-inhibited cytochrome BC1 complex with (PDB ID: 4PD4) was downloaded from the RCSB protein data bank website. Atovaquone is a drug that inhibits the respiratory chain of *Plasmodium falciparum*, but with serious limitations like known resistance, low bioavailability and high plasma protein binding [69]. cyt bc1 inhibitors are generally classified as slow-onset anti-malarials, we found that a single dose of endochin-like quinolone-400 (ELQ-400) rapidly induced stasis in blood-stage parasites, which was associated with a rapid reduction in parasitemia in vivo. ELQ-400 also exhibited a low propensity for drug resistance and was active against atovaquone-resistant *P. falciparum* strains with point mutations in cyt bc1. ELQ-400 shows that cyt bc1 inhibitors can function as single-dose, blood-stage anti-malarials and is the first compound to provide combined treatment, prophylaxis, and transmission blocking activity for malaria after a single oral administration [70]. This remarkable efficacy suggests that metabolic therapies, including cyt bc1 inhibitors, may be valuable additions to the collection of single-dose anti-malarials in current development. All docking calculations were performed on AutoDock4.2 [71], Auto Dock-Vina software [72] and as in literature [73]. The amino acids of the receptor Tyr275, Asn96, Asn271 forms H-bond with OH group and other electrostatic interactions are detailed in Fig.10. The docked ligand forms a stable complex with the receptors atovaquone-inhibited cytochrome BC1 complex as depicted in Fig.11 and the binding free energy value is -9.1 kcal/mol (Table 9). The docked ligand is embedded with the catalytic site of cytochrome BC1 complex as shown in Fig.12. These preliminary results suggest that the compound having inhibitory activity against the antimalarial receptor atovaquone-inhibited cytochrome BC1 complex. Thus, the title compound can be developed as drug used for the treatment of malaria.

5 Conclusions

The vibrational spectroscopic studies of 3-[(4-carboxyphenyl) carbamoyl]-4-hydroxy-2-oxo-1, 2-dihydroquinoline-6-carboxylic acid in the ground state were reported theoretically and experimentally. Potential energy distribution of normal mode vibration was done using GAR2PED programme. The vibrational wave number of the title compound successfully analysed. For the title compound HOMO is delocalized over the phenyl group, amide group and LUMO is over the entire molecule except carboxyl group of quinoline ring. In addition to that the halogen substituted HOMO-LUMO calculation showed a decrease in the electrophilicity index and is minimum for substituted chlorine at the eight position of the compound. The molecular electrostatic potential analysis results that the negative charge covers part of the oxygen atom in carboxylic acid and positive charge over the nitrogen atom in the quinoline ring. NBO analysis predicts a strong interactions $LPO_{37} \rightarrow C_{35}-O_{36}$, $LPO_{36} \rightarrow C_{35}-O_{37}$, $LPO_{33} \rightarrow C_{31}-O_{32}$, $LPO_{32} \rightarrow C_{31}-O_{33}$, $LPN_{20} \rightarrow C_{18}-O_{19}$, $LPO_{15} \rightarrow C_{13}-C_{14}$, $LPN_{10} \rightarrow C_{12}-O_{16}$, $LPC_4 \rightarrow C_{13}-C_{14}$ and $LPC_4 \rightarrow C_5-C_6$. The calculated first hyperpolarizability of the material is 121.75 times greater than the standard NLO material, so we can say that the compound is optically active. By DFT calculations we were able to calculate the ALIE values, beside benzene ring, we have determined H_{11} , H_{17} , H_{34} , H_{38} , H_{39} are prone to electrophilic attacks. Thanks to the mapping of the Fukui function values to the electron density surface we have also determined that carbon atom C_{21} and O_{16} , O_{36} , O_{37} are important reactive centres. Calculation of BDE showed that title molecule is not sensitive in the water surroundings towards auto oxidation mechanisms. The presence of hydrogen atoms in the RDF shows the low stability of the title compound in the degradation processes. The MD calculations of solubility parameter suggests that it is reasonable to consider Maltose as an excipient for CPCHODQ6C molecule. By molecular docking the compound form a stable complex with ubiquinol-cytochrome-c reductase inhibitor as is evident from the binding affinity values.

Acknowledgments

Part of this work has been performed with the support from Schrödinger Inc. Authors would like to extend their appreciation to the department of physics, University of Novi Sad for the Molecular dynamics simulations.

References

- [1] M. Kidway, K. R. Bhushan, P. Sapra, R. K. Saxena, R. Guptha, Alumina-supported of antibacterial quinolines used microwaves, *Bioorg. Med. chem.* 8 (2000) 69-72.
- [2] S. Tewari, P. M. S. Chauhan, A. P. Bhaduri, M. Fatima, R. K. Chatterji, Synthesis and Anti filarial agents *Bioorg. Med. Chem. Lett.* 10 (2000) 1409-1412.
- [3] T. Narendar, S. K. Tanvir, M. S. Rao, K. Srivastava, S. K. Puri Prenylated chalcones isolated from *Crotalaria* genus inhibits invitro growth of human malaria parasite *plasmodium falciparum* *Bioorg. Med. Chem. Lett.* 15 (2005) 2453-2455.
- [4] R. F Hector An overview of anti-fungal drugs and their use for treatments of deep and superficial mycoses in animals, *Clin. Tech. Small Anim. Pract.* 20 (2005) 240-249.
- [5] K. M. Khan, Z. S. Saify, Z. A. Khan, M. Ahmed, M. Saeed, M. Schick, H. J. Kohlbaun, W. Voelter, Antibiotics, Antiviral drugs, chemotherapeutics. cytostatics-syntheses and cytotoxic antimicrobial, antifungal and cardiovascular activity of new quinoline derivatives, *Arzheim. Forsch-Drug Res.* 50 (2000) 915-924.
- [6] A. Nayyar, A. Malde, E. Coutinho, R. Jain, Synthesis, anti-tuberculosis activity and 3D-QSAR study of ring-substituted-2/4-quinoline carbaldehyde derivatives, *Bioorg. Med. Chem.* 14 (2006) 7302-7310.
- [7] B. Sureshkumar, Y. Sheena Mary, C. Yohannan Panicker, K. S. Resmi, S. Suma, Stevan Armarković, Sanja J. Armarković, and C. Van Alsenoy. Spectroscopic analysis of 8-hydroxyquinoline-5-sulphonic acid and investigation of its reactive properties by DFT and molecular dynamics simulations. *J. Mol. Struct.* 1150 (2017) 540-552.
- [8] G. Bandoli, A. Dolmella, F. Tisato, M. Porchia, F. Refosco Mononuclear six coordinated Ga (III) complexes, a comprehensive survey *Coord. Chem. Rev.* 253 (2009) 56-77.
- [9] L. E. Scott, C. Orvig, Medicinal inorganic chemistry approaches to passivation and removal of aberrant metal ions in disease *Chem. Rev.* 109 (2009) 4885-4910.
- [10] M. J. Hannon, Metal based anticancer drugs, from a past anchored in platinum chemistry to a post genomic future of diverse chemistry and biology *Pure Appl. Chem.* 79 (2007) 2243-2261.
- [11] R. T. Ulahannan, C. Y. Panicker, H. T. Varghese, R. Musiol, J. Jampilek, C. Van Alsenoy, J. A. War, S. K. Srivastava, Molecular structure, FT-IR, FT-Raman, NBO, HOMO and LUMO, MEP, NLO and molecular docking study of 2-[(E)-2-(2-

- bromophenyl)-ethenyl quinoline-6-carboxylic acid *Spectrochim. Acta.* 151 (2015) 184-197.
- [12] E. Fazal, C. Y. Panicker, H. T. Varghese, S. Nagarajan, B. S. Sudha, J. A. War, S. K. Srivastava, S. B. Harikumar, P. L. Anto, Vibrational spectroscopic and molecular docking study of 4-methylphenylquinoline-2-carboxylate *Spectrochim. Acta* 143 (2015) 213-222.
- [13] S. A. Khan, A. M. Asiri, S. H. Al-Thaqafy, H. M. F. Aidallah, S. A. El-Daly, Synthesis, characterization and spectroscopic behavior of novel 2-oxo-1,4-disubstituted-1,2,5,6-tetrahydrobenzo[h]quinoline-3-carbonitrildyes, *Spectrochim. Acta* 133 (2014) 141-148.
- [14] C. B. Sangani, J. A. Makawana, X. Zhang, S. C. Teraiya, I. Lin, H. L. Zhu, Design, synthesis and molecular modeling of pyrazole-quinoline-pyridine hybrids as a new class of antimicrobial and anticancer agents, *Eur. J. Med. Chem.* 76 (2014) 549-557.
- [15] L. Strekowski, J. L. Mokrosz, A. H. Vidya, A. Czarny, M. T. Cegla, R. L. Wydra, S. E. Patterson, R. S. Schinazi, Synthesis and quantitative structure- Activity relationship analysis of 2-(aryl or heteroaryl) quinoline-4-amines a new class of anti-HIV-1agents, *J. med. Chem.* 34 (1991) 1739-1746.
- [16] S. Armakovic, S. J. Armakovic, J.P. Setrajcic, I. J. Serajcic, Active components of frequently used β - blockers from the aspect of computational study. *J. Mol. Model* 18 (2012) 4491-4501.
- [17] D. J. Greenhalgh, A. C. Williams, P. Timmins, P. York, Solubility parameters as predictors of miscibility in solid dispersions, *J. Pharm. Sci.* 88 (1999) 1182-1190.
- [18] R. C. Rowe, Adhesion of film coatings to tablet surfaces-a theoretical approach based on solubility parameters, *Int. J. Pharm.* 41 (1988) 219-222.
- [19] R.C. Rowe, Interactions in coloured powders and tablet formulations: a theoretical approach based on solubility parameters, *Int. J. Pharm.* 53 (1989) 47-51.
- [20] J. Jampilek, R. Musiol, M. Pesko, K. Kralova, M. Vejsova, J. Carroll, A. Coffey, J. Finster, D. Tabak, H. Niedbala, V. Kozik, J. Polanski, J. Dohnal, Ring-substituted 4-hydroxy-1H-quinolin-2-ones: Preparation and biological activity. *Molecules*, 14 (2009) 11451159.
- [21] Gaussian 09, Revision B.01, M. J. Frisch, G. W. Trucks, H. B. Schlegel, G. E. Scuseria, M.A. Robb, J. R. Cheeseman, G. Scalmani, V. Barone, B. Mennucci, G. A. Petersson, H. Nakatsuji, M. Caricato, X. Li, H. P. Hratchian, A. F. Izmaylov, J.

- Bloino, G. Zheng, J. L. Sonnenberg, M. Hada, M. Ehara, K. Toyota, R. Fukuda, J. Hasegawa, M. Ishida, T. Nakajima, Y. Honda, O. Kitao, H. Nakai, T. Vreven, J. A. Montgomery, Jr., J. E. Peralta, F. Ogliaro, M. Bearpark, J. J. Heyd, E. Brothers, K. N. Kudin, V. N. Staroverov, T. Keith, R. Kobayashi, J. Normand, K. Raghavachari, A. Rendell, J. C. Burant, S. S. Iyengar, J. Tomasi, M. Cossi, N. Rega, J. M. Millam, M. Klene, J. E. Knox, J. B. Cross, V. Bakken, C. Adamo, J. Jaramillo, R. Gomperts, R.E. Stratmann, O. Yazyev, A. J. Austin, R. Cammi, C. Pomelli, J. W. Ochterski, R. L. Martin, K. Morokuma, V. G. Zakrzewski, G. A. Voth, P. Salvador, J. J. Dannenberg, S. Dapprich, A. D. Daniels, O. Farkas, J. B. Foresman, J. V. Ortiz, J. Cioslowski, and D. J. Fox, Gaussian, Inc., Wallingford CT, 2010.
- [22] J. B. Foresman, in: E. Frisch (Ed.), *Exploring Chemistry with Electronic Structure Methods: A Guide to Using Gaussian*, Gaussian Inc., Pittsburg, PA, 1996.
- [23] Gauss View, Version 5, R. Dennington, T. Keith, J. Millam, Semichem Inc., Shawnee Mission, KS, 2009.
- [24] J. M. L. Martin, C. Van Alsenoy, GAR2PED, A Program to Obtain a Potential Energy Distribution from a Gaussian Archive Record, University of Antwerp, Belgium, 2007.
- [25] A. D. Becke, Density-functional thermochemistry. III. The role of exact exchange, *J. Chem. Phys.* 98(7) (1993) 5648-5652.
- [26] J. L. Banks, H.S. Beard, Y. Cao, A.E. Cho, W. Damm, R. Farid, A.K. Felts, T.A. Halgren, D.T. Mainz, J.R. Maple, Integrated modeling program, applied chemical theory (IMPACT), *J. Comput. Chem.* 26(16) (2005) 1752-1780.
- [27] H. J. Berendsen, J. P. Postma, W. F. van Gunsteren, J. Hermans, Interaction models for water in relation to protein hydration, in *Intermolecular forces*. 1981, Springer. p. 331-342.
- [28] Schrödinger Release 2015-4: Maestro, version 10.4, Schrödinger, LLC, New York, NY, 2015. 2015.
- [29] J. Chowdhury, M. Ghosh, T.N. Misra, Surface enhanced Raman scattering of 2,2-biquinoline adsorbed on colloidal silver particles, *Spectrochim. Acta* 56 (2000) 2107-2115.
- [30] R. T. Ulahannan, C. Y. Panicker, H. T. Varghese, C. Van Alsenoy, R. Musiol, J. Jampilek, P. L. Anto Spectroscopic (FT-IR, FT-Raman) investigations and quantum chemical calculations of 4-hydroxy-2-oxo-1,2-dihydroquinoline-7-carboxylic acid *Spectrochim. Acta* 121 (2014) 404-414.

- [31] N. P. G. Roeges, *A Guide to the Complete Interpretation of the Infrared spectra of Organic Compounds*, Wiley, New York 1994.
- [32] G. Varsanyi, *Assignments of Vibrational Spectra of Seven Hundred Benzene Derivatives*, Wiley, New York 1974.
- [33] N. B. Colthup, L. H. Daly, S. E. Wiberly, *Introduction to IR and Raman Spectroscopy*, Academic Press, New York, 1990.
- [34] R. M. Silverstein, F. X. Webster, *Spectrometric Identification of Organic Compounds*, ED. 6, John Wiley, Asia, 2003.
- [35] C. Y. Panicker, H. T. Varghese, A. John, D. Philip, H. I. S. Nogueira, Vibrational spectra of melamine diborate, $C_3N_6H_6_2H_3BO_3$, *Spectrochim. Acta* 58 (2002) 1545-1551.
- [36] Y. S. Mary, P. J. Jojo, C. Van Alsenoy, M. Kaur, M. S. Siddegowda, H. S. Yathirajan, H. I. S. Nogueira, S. M. A. Cruz, Vibrational spectroscopic studies (FT-IR, FT-Raman, SERS) and quantum chemical calculations on cyclobenzaprinium salicylate, *Spectrochim. Acta* 120 (2014) 340-350.
- [37] L. J. Bellamy, *The IR spectra of Complex Molecules*, John Wiley and Sons, New York 1975.
- [38] S. H. R. Sebastian, M. A. Al-Alshaikh, A. A. El-Emam, C. Y. Panicker, J. Zitko, M. Dolezal, C. Van Alsenoy, Spectroscopic quantum chemical studies, Fukui functions, in vitro antiviral activity and molecular docking of 5-chloro-N-(3-nitrophenyl) pyrazine-2-carboxamide, *J. Mol. Struct.* 1119 (2016) 188-199.
- [39] V. V. Menon, E. Foto, Y. S. Mary, E. Karatas, C. Y. Panicker, G. Yalcin, S. Armakovic, S. J. Armakovic, C. Van Alsenoy, I. Yildiz, Vibrational spectroscopic analysis, molecular dynamics simulations and molecular docking study of 5-nitro-2-phenoxyethyl benzimidazole, *J. Mol. Struct.* 1129 (2017) 86-97.
- [40] G. Socrates, *Infrared Characteristic Group Frequencies*, John Wiley and Sons, New York, 1981.
- [41] V. S. Madhvan, H. T. Varghese, S. Mathew, J. Vinsova, C. Y. Panicker, FT-IR, FT-Raman and DFT calculations of 4-Chloro-2-(3,4-dichlorophenyl carbamoyl) phenyl acetate, *Spectrochim. Acta.* 72 (2009) 547-553
- [42] C. Y. Panicker, K. R. Ambujakshan, H. T. Varghese, S. Mathew, S. Ganguli, A. K. Nanda, C. Van Alsenoy, FT-IR, FT-Raman and DFT calculations of 3-[(4-fluorophenyl)methylene]amino}-2-phenylquinazolin-4(3H)-one, *J. Raman. Spectrosc.* 40 (2009) 527-536.

- [43] A. S. El-Azab, Y. S. Mary, C. Y. Panicker, A. A.-M A-Aziz, A. Magda, El-Sherbeny, C. V. Alsenoy, DFT and experimental (FT-IR and FT-Raman) investigation of vibrational spectroscopy and molecular docking studies of 2-(4-oxo-3-phenyl-3,4-dihydroquinazolin-2-ylthio)-N-(3,4,5 trimethoxy phenyl) acetamide, *J. Mol. Struct.* 1113 (2016) 133-145.
- [44] F. J. Luque, J. M. Lopez, M. Orozco, Perspective on electrostatic interactions of a solute with a continuum, a direct utilization of ab initio molecular potentials for the prevision of solvent effects, *Theor. Chem. Acc.* 103 (2000) 343-345.
- [45] P. Politzer, J. S. Murray, in: D.L. Beveridge, R. Lavery, (Eds.), *Theoretical Biochemistry and Molecular Biophysics*, Springer, Berlin, 1991.
- [46] NBO Version 3.1, E.D. Glendening, A.E. Reed, J.E. Carpenter, F. Weinhold.
- [47] C. Adant, M. Dupuis, J. L. Bredas, Ab initio study of the nonlinear optical properties of urea, electron correlation and dispersion effects, *Int. J. Quantum. Chem.* 56 (1995) 497-507.
- [48] G. Purohit, G. C. Joshi, Second order polarizabilities of some quinolines, *Indian J. Pure Appl. Phys.* 41 (2003) 922-927.
- [49] Y. S. Mary, C. Y. Panicker, H. T. Varghese, K. Raju, T. E. Bolelli, I. Yildiz, C. M. Granadeiro, H. I. S. Nogueira, Vibrational spectroscopic studies and computational study of 4-fluoro-N-(2'-hydroxy-4'-nitrophenyl) phenylacetamide, *J. Mol. Struct.* 994 (2011) 223-231.
- [50] S. R. Sheeja, N. A. Mangalam, M. R. P. Kurup, Y. S. Mary, K. Raju, H. T. Varghese, C. Y. Panicker, Vibrational spectroscopic studies and computational study of quinoline-2-carbaldehyde benzyol hydrazone, *J. Mol. Struct.* 973 (2010) 36-46.
- [51] J. S. Murray, J.M. Seminario, P. Politzer, P. Sjoberg, Average local ionization energies computed on the surfaces of some strained molecules, *Int. J. Quantum Chem.* 38(S24) (1990) 645-653.
- [52] P. Politzer, F. Abu-Awwad, J.S. Murray, Comparison of density functional and Hartree-Fock average local ionization energies on molecular surfaces, *Int. J. Quantum Chem.* 69(4) (1998) 607-613.
- [53] A. Toro-Labb, P. Jaque, J. S. Murray, P. Politzer, Connection between the average local ionization energy and the Fukui function, *Chem. Phys. Lett.* 407 (2005) 143-146.
- [54] R. G. Parr, *Density Functional Theory of Atoms and Molecules*, in *Horizons of Quantum Chemistry*, Springer, (1980) 5-15.

- [55] A. Michalak, F. De Proft, P. Geerlings, R. Nalewajski, Fukui functions from the relaxed Kohn-Sham orbitals, *J. Phys. Chem. A* 103 (1999) 762-771.
- [56] X. Ren, Y. Sun, X. Fu, L. Zhu, Z. Cui, DFT comparison of the OH-initiated degradation mechanisms for five chlorophenoxy herbicides, *J. Mol. Model.* 19 (2013) 2249-2263.
- [57] I. Ai, J. Y. Liu, Mechanism of OH-initiated atmospheric oxidation of E/Z-CF₃CF=CF₃: a quantum mechanical study, *J. Mol. Model.* 20 (2014) 1-10.
- [58] W. Sang-aroon, V. Amornkitbamrung, V. Ruangpornvisuti, A density functional theory study on peptide bond cleavage at aspartic residues: direct vs cyclic intermediate hydrolysis, *J. Mol. Model.* 19 (2013) 5501-5513.
- [59] J. Kieffer, É. Brémond, P. Lienard, G. Boccardi, In silico assessment of drug substances chemical stability, *J. Mol. Struct. THEOCHEM.* 954 (2010) 75-79.
- [60] J. S. Wright, H. Shadnia, L. L. Chepelev, Stability of carbon-centered radicals: Effect of functional groups on the energetics of addition of molecular oxygen, *J. Comput. Chem.* 30 (2009) 1016-1026.
- [61] P. Lienard, J. Gavartin, G. Boccardi, M. Meunier, Predicting drug substances autoxidation, *Pharm. Res.* 32(1) (2015) 300-310.
- [62] T. Andersson, A. Broo, E. Evertsson, Prediction of Drug Candidates' Sensitivity Toward Autoxidation: Computational Estimation of C-H Dissociation Energies of Carbon-Centered Radicals, *J. Pharm. Sci.* 103 (7) (2014) 1949-1955.
- [63] R. V. Vaz, J. R. Gomes, C. M. Silva, Molecular dynamics simulation of diffusion coefficients and structural properties of ketones in supercritical CO₂ at infinite dilution, *J. Supercritic. Fluids*, 107 (2016) 630-638.
- [64] M. Cunha-Rodrigues, M. Prudencio, M. M. Mota, W. Haas, Antimalarial drugs–host targets (re)visited, *Biotechnol. J.* 1 (2006) 321-332.
- [65] C. Daneshvar, T. M. Davis, J. Cox-Singh, M. Z. Rafa'ee, S. K. Zakaria, P. C. Divis, B. Singh, Clinical and laboratory features of human Plasmodium knowlesi infection, *Clin. Infect. Dis.* 49 (2009) 852-860.

- [66] B. Gunsaru, S. J. Burgess, W. Morrill, J. X. Kelly, S. Shomloo, M. J. Smilkstein, K. Liebman, D. H. Peyton, Simplified reversed chloroquinines to overcome malaria resistance to quinoline-based drugs, *Antimicrob. Agents Chemother.* 61 (2017) 1913-1916.
- [67] B. Sandhya, S. Kumar, S. Drabu, R. Kumar, Structural modifications of quinoline-based antimalarial agents: Recent developments, *J. Pharm. Bioallied. Sci.* 2 (2010) 64-71.
- [68] A. Lagunin, A. Stepanchikova, D. Filimonov, V. Poroikov, PASS: prediction of activity spectra for biologically active substances, *Bioinformatics* 16 (2000) 747-748.
- [69] A. C. R. Sodero, B. Abraham-Vieira, P. H. M. Torres, P. G. Pascutti, C. R. S. Garcia, V. F. Ferreira, D. R. da Rocha, S. B. Ferreira, F. P. Silva, Atovaquone is a drug that inhibits the respiratory chain of *Plasmodium falciparum*, but with serious limitations like known resistance, low bioavailability and high plasma protein binding, *Mem. Inst. Oswaldo. Cruz*, 112 (2017) 299-308.
- [70] A. M. Stickles, L. M. Ting, J. M. Morrissey, Y. Li, M. W. Mather, E. Meermeier, A. M. Pershing, I. P. Forquer, G. P. Miley, S. Pou, R. W. Winter, D. J. Hinrichs, J. X. Kelly, K. Kim, A. B. Vaidya, M. K. Riscoe, A. Nilsen, Inhibition of Cytochrome bc1 as a Strategy for Single-Dose, Multi-Stage Antimalarial Therapy, *Am. J. Trop. Med. Hyg.* 92 (2015) 1195-1201.
- [71] G. M. Morris, R. Huey, W. Lindstrom, M. F. Sanner, R. K. Belew, D. S. Goodsell, A. J. Olson, Autodock4 and AutoDockTools4: automated docking with selective receptor flexibility, *J. Comput. Chem.* 16 (2009) 2785-2791.
- [72] O. Trott, A. J. Olson, "AutoDock Vina: Improving the speed and accuracy of docking with a new scoring function, efficient optimization and multithreading," *J. Comput. Chem.* 31 (2010) 455-461.
- [73] J. A. War, K. Jalaja, Y. S. Mary, C. Y. Panicker, S. Armakovic, S. J. Armakovic, S. K. Srivastava, C. Van Alsenoy, Spectroscopic characterization of 1-[3-(1H-imidazol-1-yl)propyl]-3-phenylthiourea and assessment of reactive and optoelectronic properties employing DFT calculations and molecular dynamics simulations, *J. Mol. Struct.* 1129 (2017) 72-85.

Figure Caption

Fig 1 FT-IR

Fig 2 FT-Raman

Fig 3 Molecule

Fig 4 HOMO-LUMO

Fig 5 MEP

Fig 6 ALIE

Fig 7 Fukui

Fig 8 BDE

Fig 9 RDF

Fig 10 Docking

Fig 11 Docking

Fig 12 Docking

Table Caption

Table 1 Geometrical Parameters

Table 2 Frequency

Table 3 HOMO-LUMO

Table 4 NBO-1

Table 5 NBO-2

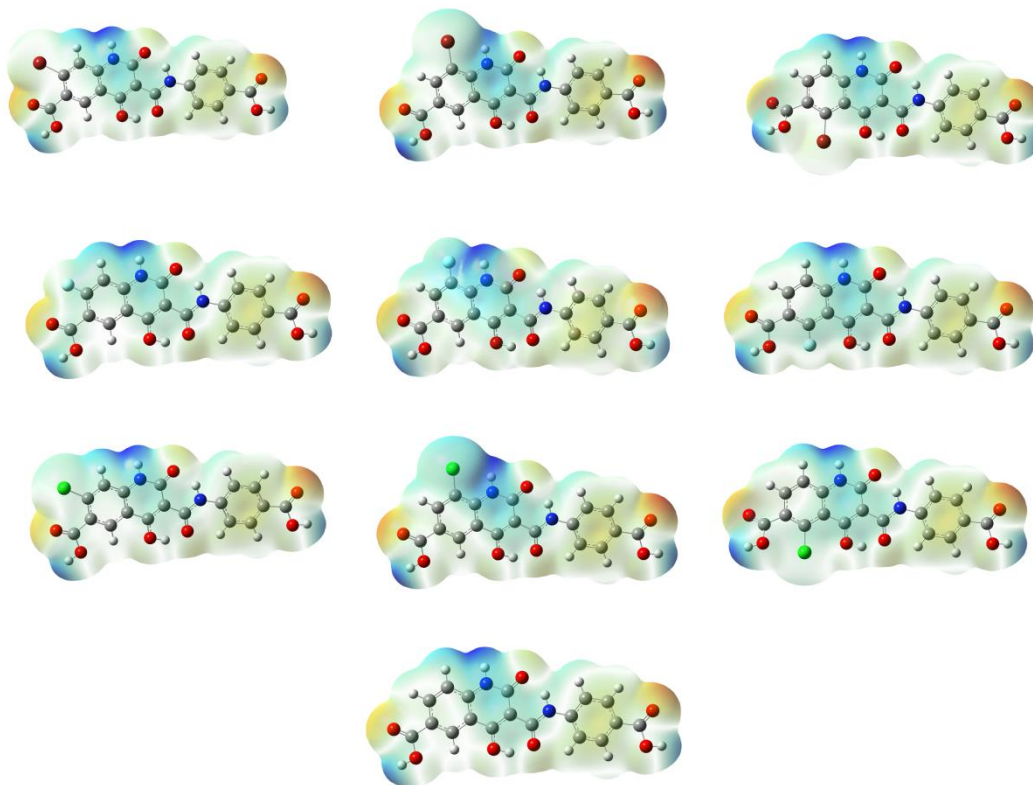
Table 6 NLO of Substitution

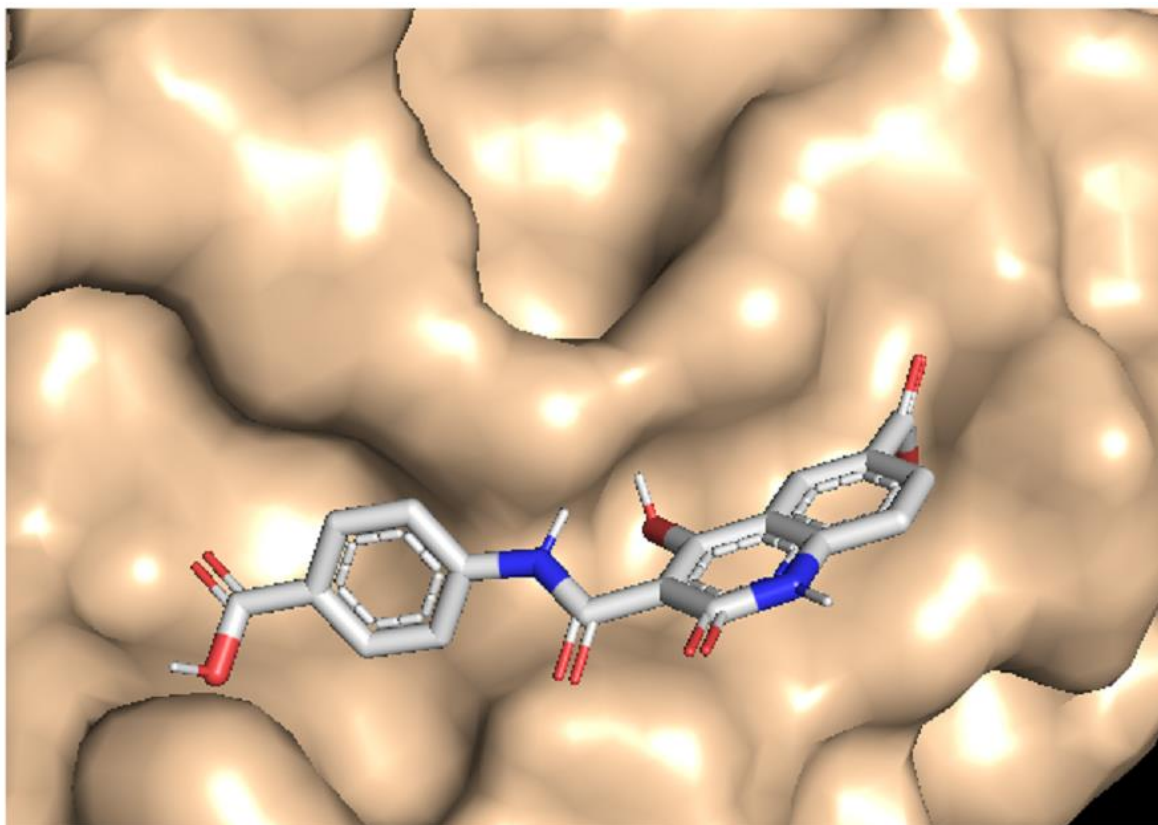
Table 7 Solubility parameter

Table 8 Pass Analysis

Table 9 Docking

Graphical Abstract





Tables

Table 1

Optimized Geometrical parameters of 3-[(4-carboxyphenyl) carbamoyl] -4-hydroxy-2-oxo-1, 2-dihydroquinoline-6-carboxylic acid.

Bond length (Å)		Bond angle (°)		Dihedral angle (°)	
C ₁ -C ₂	1.3824	C ₂ -C ₁ -C ₆	120.9	C ₆ -C ₁ -C ₂ -C ₃	-0.0
C ₁ -C ₆	1.4113	C ₂ -C ₁ -H ₇	120.8	C ₂ -C ₁ -C ₆ -C ₅	-0.0
C ₁ -H ₇	1.0863	C ₁ -C ₂ -C ₃	119.6	C ₂ -C ₁ -C ₆ -C ₃₅	180.0
C ₂ -C ₃	1.4084	C ₁ -C ₂ -H ₈	120.7	C ₁ -C ₂ -C ₃ -C ₄	0.0
C ₂ -H ₈	1.0880	C ₆ -C ₁ -H ₇	118.3	C ₁ -C ₂ -C ₃ -N ₁₀	180.0
C ₃ -C ₄	1.4130	C ₁ -C ₆ -C ₅	119.6	C ₂ -C ₃ -C ₄ -C ₅	0.0

C ₃ -N ₁₀	1.3745	C ₁ -C ₆ -C ₃₅	117.8	C ₂ -C ₃ -C ₄ -C ₁₃	-180.0
C ₄ -C ₅	1.4045	C ₃ -C ₂ -H ₈	119.7	N ₁₀ -C ₃ -C ₄ -C ₅	-180.0
C ₄ -C ₁₃	1.4498	C ₂ -C ₃ -C ₄	120.1	N ₁₀ -C ₃ -C ₄ -C ₁₃	0.0
C ₅ -C ₆	1.3916	C ₂ -C ₃ -N ₁₀	121.3	C ₂ -C ₃ -N ₁₀ -C ₁₂	-180.0
C ₅ -H ₉	1.0841	C ₄ -C ₃ -N ₁₀	118.6	C ₄ -C ₃ -N ₁₀ -C ₁₂	0.0
C ₆ -C ₃₅	1.4849	C ₃ -C ₄ -C ₅	119.5	C ₃ -C ₄ -C ₅ -C ₆	-0.0
N ₁₀ -H ₁₁	1.0127	C ₃ -C ₄ -C ₁₃	118.4	C ₁₃ -C ₄ -C ₅ -C ₆	180.0
N ₁₀ -C ₁₂	1.3914	C ₃ -N ₁₀ -H ₁₁	119.9	C ₃ -C ₄ -C ₁₃ -C ₁₄	-0.0
C ₁₂ -C ₁₄	1.4579	C ₃ -N ₁₀ -C ₁₂	126.0	C ₃ -C ₄ -C ₁₃ -O ₁₅	-180.0
C ₁₂ -O ₁₆	1.2374	C ₅ -C ₄ -C ₁₃	122.1	C ₅ -C ₄ -C ₁₃ -C ₁₄	180.0
C ₁₃ -C ₁₄	1.3989	C ₄ -C ₅ -C ₆	120.3	C ₅ -C ₄ -C ₁₃ -O ₁₅	-0.0
C ₁₃ -O ₁₅	1.3198	C ₄ -C ₅ -H ₉	119.0	C ₄ -C ₅ -C ₆ -C ₁	0.0
C ₁₄ -C ₁₈	1.4854	C ₄ -C ₁₃ -C ₁₄	121.2	C ₄ -C ₅ -C ₆ -C ₃₅	-180.0
O ₁₅ -H ₁₇	1.0122	C ₄ -C ₁₃ -O ₁₅	115.9	C ₁ -C ₆ -C ₃₅ -O ₃₆	0.0
O ₁₆ -H ₃₉	1.7992	C ₆ -C ₅ -H ₉	120.7	C ₁ -C ₆ -C ₃₅ -O ₃₇	180.0
H ₁₇ -O ₁₉	1.5785	C ₅ -C ₆ -C ₃₅	122.5	C ₅ -C ₆ -C ₃₅ -O ₃₆	-180.0
C ₁₈ -O ₁₉	1.2507	C ₆ -C ₃₅ -O ₃₆	124.7	C ₅ -C ₆ -C ₃₅ -O ₃₇	-0.0
C ₁₈ -N ₂₀	1.3596	C ₆ -C ₃₅ -O ₃₇	113.0	C ₃ -N ₁₀ -C ₁₂ -C ₁₄	-0.0
N ₂₀ -C ₂₁	1.4047	H ₁₁ -N ₁₀ -C ₁₂	114.0	C ₃ -N ₁₀ -C ₁₂ -O ₁₆	180.0
N ₂₀ -H ₃₉	1.0244	N ₁₀ -C ₁₂ -C ₁₄	116.0	N ₁₀ -C ₁₂ -C ₁₄ -C ₁₃	0.0
C ₂₁ -C ₂₂	1.4068	N ₁₀ -C ₁₂ -O ₁₆	118.0	N ₁₀ -C ₁₂ -C ₁₄ -C ₁₈	180.0
C ₂₁ -C ₂₃	1.4092	C ₁₄ -C ₁₂ -O ₁₆	126.0	O ₁₆ -C ₁₂ -C ₁₄ -C ₁₃	-180.0
C ₂₂ -C ₂₄	1.3924	C ₁₂ -C ₁₄ -C ₁₃	119.8	O ₁₆ -C ₁₂ -C ₁₄ -C ₁₈	0.0
C ₂₂ -H ₂₅	1.0814	C ₁₂ -C ₁₄ -C ₁₈	122.1	C ₄ -C ₁₃ -C ₁₄ -C ₁₂	-0.0
C ₂₃ -C ₂₆	1.3864	C ₁₂ -C ₁₆ -H ₃₉	99.6	C ₄ -C ₁₃ -C ₁₄ -C ₁₈	-180.0
C ₂₃ -H ₂₇	1.0896	C ₁₄ -C ₁₃ -O ₁₅	123.0	O ₁₅ -C ₁₃ -C ₁₄ -C ₁₂	180.0

C ₂₄ -C ₂₈	1.4017	C ₁₃ -C ₁₄ -C ₁₈	118.1	O ₁₅ -C ₁₃ -C ₁₄ -C ₁₈	0.0
C ₂₄ -H ₂₉	1.0859	C ₁₃ -O ₁₅ -H ₁₇	106.1	C ₁₂ -C ₁₄ -C ₁₈ -O ₁₉	180.0
C ₂₆ -C ₂₈	1.4030	C ₁₄ -C ₁₈ -O ₁₉	120.2	C ₁₂ -C ₁₄ -C ₁₈ -N ₂₀	0.0
C ₂₆ -H ₃₀	1.0863	C ₁₄ -C ₁₈ -N ₂₀	116.8	C ₁₃ -C ₁₄ -C ₁₈ -O ₁₉	0.0
C ₂₈ -C ₃₁	1.4815	O ₁₅ -H ₁₇ -O ₁₉	149.6	C ₁₃ -C ₁₄ -C ₁₈ -N ₂₀	180.0
C ₃₁ -O ₃₂	1.2132	O ₁₉ -C ₁₈ -N ₂₀	123.0	C ₁₄ -C ₁₈ -N ₂₀ -C ₂₁	-180.0
C ₃₁ -O ₃₃	1.3596	C ₁₈ -O ₁₉ -H ₁₇	103.1	O ₁₉ -C ₁₈ -N ₂₀ -C ₂₁	0.0
O ₃₃ -H ₃₄	0.9720	C ₁₈ -N ₂₀ -C ₂₁	129.2	C ₁₈ -N ₂₀ -C ₂₁ -C ₂₂	-0.0
C ₃₅ -O ₃₆	1.2120	C ₁₈ -N ₂₀ -H ₃₉	113.5	C ₁₈ -N ₂₀ -C ₂₁ -C ₂₃	180.0
C ₃₅ -O ₃₇	1.3554	C ₂₁ -N ₂₀ -H ₃₉	117.3	N ₂₀ -C ₂₁ -C ₂₂ -C ₂₄	-180.0
O ₃₇ -H ₃₈	0.9722	N ₂₀ -C ₂₁ -C ₂₂	124.3	C ₂₃ -C ₂₁ -C ₂₂ -C ₂₄	0.0
		N ₂₀ -C ₂₁ -C ₂₃	116.3	N ₂₀ -C ₂₁ -C ₂₃ -C ₂₆	180.0
		N ₂₀ -H ₃₉ -O ₁₆	141.9	C ₂₂ -C ₂₁ -C ₂₃ -C ₂₆	-0.0
		C ₂₂ -C ₂₁ -C ₂₃	119.4	C ₂₁ -C ₂₂ -C ₂₄ -C ₂₈	0.0
		C ₂₁ -C ₂₂ -C ₂₄	119.5	C ₂₁ -C ₂₃ -C ₂₆ -C ₂₈	0.0
		C ₂₁ -C ₂₂ -H ₂₅	119.7	C ₂₂ -C ₂₄ -C ₂₈ -C ₂₆	-0.0
		C ₂₁ -C ₂₃ -C ₂₆	120.5	C ₂₂ -C ₂₄ -C ₂₈ -C ₃₁	180.0
		C ₂₁ -C ₂₃ -H ₂₇	119.5	C ₂₃ -C ₂₆ -C ₂₈ -C ₂₄	0.0
		C ₂₄ -C ₂₂ -H ₂₅	120.8	C ₂₃ -C ₂₆ -C ₂₈ -C ₃₁	-180.0
		C ₂₂ -C ₂₄ -C ₂₈	121.2	C ₂₄ -C ₂₈ -C ₃₁ -O ₃₂	180.0
		C ₂₂ -C ₂₄ -H ₂₉	119.4	C ₂₄ -C ₂₈ -C ₃₁ -O ₃₃	-0.0
		C ₂₆ -C ₂₃ -H ₂₇	120.0	C ₂₆ -C ₂₈ -C ₃₁ -O ₃₂	0.0
		C ₂₃ -C ₂₆ -C ₂₈	120.4	C ₂₆ -C ₂₈ -C ₃₁ -O ₃₃	180.0
		C ₂₃ -C ₂₆ -H ₃₀	120.8		
		C ₂₈ -C ₂₄ -H ₂₉	119.5		
		C ₂₄ -C ₂₈ -C ₂₆	119.1		

		C ₂₄ -C ₂₈ -C ₃₁	122.8		
		C ₂₈ -C ₂₆ -H ₃₀	118.8		
		C ₂₆ -C ₂₈ -C ₃₁	118.2		
		C ₂₈ -C ₃₁ -O ₃₂	125.2		
		C ₂₈ -C ₃₁ -O ₃₃	113.1		
		O ₃₂ -C ₃₁ -O ₃₃	121.7		
		C ₃₁ -O ₃₃ -H ₃₄	105.8		
		O ₃₆ -C ₃₅ -O ₃₇	122.3		
		C ₃₅ -O ₃₇ -H ₃₈	106.2		

Table 2

Calculated scaled wavenumbers, observed IR, Raman bands and vibrational assignments with potential energy distribution (PED) of CPCHODQ6C.

B3LYP/6-31G*			IR(cm ⁻¹)	Raman(cm ⁻¹)	Assignments
v(cm ⁻¹)	IR _I	R _A			
3545	64.41	295.68	-	3542	vO ₃₃ H ₃₄ (99)
3545	85.56	236.91	-	-	vO ₃₇ H ₃₈ (99)
3454	50.89	108.89	3440 3392	-	vN ₁₀ H ₁₁ (100)
3231	398.20	431.45	-	-	vN ₂₀ H ₃₉ (99)
3151	2.95	39.19	3157	-	vCHII(98)
3128	2.89	37.14	-	3132	vCHI(99)
3101	1.58	143.23	-	3103	vCHI(95)
3099	1.69	95.44	-	-	vCHII(95)
3098	2.12	95.49	-	-	vCHII(93)
3067	6.25	85.67	-	3078	vCHI(95)

3061	7.07	48.71	2990	-	vCHII(95)
2793	903.66	56.85	2666	-	vO ₁₅ H ₁₇ (99)
1746	362.66	269.81	-	-	vC ₃₅ O ₃₆ (73)
1741	401.29	169.61	-	-	vC ₃₁ O ₃₂ (72)
1678	512.03	10.06	1670	-	vC ₁₂ O ₁₆ (37)
1625	138.36	620.76	-	1630	vC ₁₈ O ₁₉ (26)
1618	74.61	349.28	-	-	vPhI(23)
1609	170.19	11.78	-	-	vPhII(30)
1591	978.08	1638.12	1593	1602	vPhII(24)
1580	208.84	1.94	-	-	vPhI(49)
1562	41.76	118.04	1551	1548	vC ₁₃ C ₁₄ (22), vPhI(15), δO ₁₅ H ₁₇ (10)
1538	986.10	1388.60	1505	1503	vPhII(27), δC ₁₈ O ₁₉ (13), vC ₁₄ C ₁₈ (11)
1496	26.65	130.96	-	-	vPhII(48), δCHII(45)
1485	165.35	350.03	1470	1477	vPhI(24), δCHI(20), vC ₃ N ₁₀ (11)
1439	35.79	131.12	-	-	δN ₁₀ H ₁₁ (22), vPhI(13), vC ₁₃ N ₁₀ (13)
1413	213.93	438.67	1413	1414	vC ₄ C ₁₃ (15)
1403	14.30	86.10	-	1382	vPhII(42), δCHII(27)
1369	5.58	23.41	1372	-	vPhI(51), δCHI(12), δN ₁₀ H ₁₁ (12)
1352	68.74	955.36	-	-	δO ₁₅ H ₁₇ (17), vC ₁₃ C ₁₄ (17)
1342	111.52	191.03	-	-	vPhI(26), δC ₁₈ O ₁₉ (15)
1338	67.92	1.95	-	-	δO ₃₇ H ₃₈ (12), vC ₃₅ O ₃₇ (1)
1336	473.63	189.54	-	-	δO ₃₃ H ₃₄ (13), vC ₃₁ O ₃₃ (12)
1321	60.41	257.62	1314	1323	vPhII(73)
1292	165.43	5.51	-	-	vCO(17), vN ₁₀ C ₁₂ (16), vC ₁₂ C ₁₄ (14)
1288	13.42	128.21	1284	-	δCHII(62)
1251	103.81	403.81	1261	1260	δC ₁₈ O ₁₉ (19)

1245	27.98	711.98	-	-	δ CHI(23), ν C ₂₁ N ₂₀ (16)
1233	20.23	111.26	-	-	ν C ₃ N ₁₀ (17), δ C ₁₈ O ₁₉ (19), δ N ₁₀ H ₁₁ (14)
1210	29.32	0.61	-	-	δ C ₁₈ O ₁₉ (36)
1184	195.44	11.90	-	1183	δ O ₃₃ H ₃₄ (31), δ CHII(20), δ C ₂₈ C ₃₁ (13)
1173	207.87	95.65	1173	-	δ O ₃₇ H ₃₈ (31), C ₆ C ₃₅ (13)
1152	305.17	415.54	-	-	δ CHII(48), δ O ₃₃ H ₃₄ (14)
1137	10.52	14.28	-	1134	δ CHI(42)
1106	75.21	24.52	1114	-	ν C ₁₂ N ₁₀ (12), δ CHII(12)
1104	98.68	4.34	-	1099	δ CHII(36)
1082	59.18	15.91	-	-	ν C ₁₂ N ₁₀ (15), ν C ₃₁ O ₃₃ (15)
1072	204.93	7.50	-	1070	ν PhII (36), ν C ₃₁ O ₃₃ (33)
1066	39.09	0.59	-	-	ν PhI(18), ν C ₃₅ O ₃₇ (31), δ CHII(12)
994	6.99	18.05	1014	1020	δ PhII(53), ν PhII(32)
951	0.97	3.82	-	970	γ CHII(79), γ PhII(17)
949	0.16	0.50	-	-	γ CHI(86)
948	7.70	4.16	946	-	δ C ₁₈ O ₁₉ (22), δ PhI(13)
938	0.47	0.41	-	-	γ CHII(90)
925	8.72	1.32	-	926	γ CHII(78)
922	118.10	0.48	-	-	γ O ₁₅ H ₁₇ (96)
896	7.84	16.48	-	870	δ C ₁₈ O ₁₉ (26), δ PhI(17)
846	3.44	26.96	846	-	δ C ₁₈ O ₁₉ (29), δ N ₂₀ H ₃₉ (18)
842	28.35	0.08	-	841	γ CHII(63)
828	36.23	2.99	-	-	γ CHII(67), γ N ₂₀ H ₃₉ (17)
815	9.54	3.18	-	818	γ CHI(70)
812	9.74	30.00	807	-	δ C ₁₈ O ₁₉ (41), δ ring(11)
794	38.68	1.37	-	799	γ CHII(50), γ N ₂₀ H ₃₉ (20), γ N ₂₀ C ₁₈ (15)

762	49.05	4.20	768	776	γ PhII(25), γ C ₃₁ O ₃₂ (22), γ C ₂₁ N ₂₀ (10)
759	2.41	2.35	-	-	γ ring(32), δ C ₁₃ O ₁₅ (23), γ PhI(11)
754	62.10	0.65	-	754	γ C ₃₅ O ₃₆ (41), γ PhI(15), γ CHI(11)
744	45.76	5.18	-	-	ν C ₂₈ C ₃₁ (19)
736	36.51	2.95	-	-	γ C ₁₂ O ₁₆ (29), γ C ₁₈ O ₁₉ (15), γ PhI(14)
709	18.04	22.94	-	-	δ PhII(11), δ PhI(10)
701	12.14	1.59	-	-	γ C ₁₈ O ₁₉ (29), γ ring(17), γ N ₁₀ H ₁₁ (13)
694	37.34	2.03	688	-	γ PhII(56), γ C ₂₈ C ₃₁ (13), γ C ₂₁ N ₂₀ (11)
659	9.95	2.43	-	668	γ PhI(21), δ C ₁₃ O ₁₅ (30), γ ring(10)
650	11.28	21.35	648	-	δ PhI(34), δ ring(11)
637	37.11	1.29	-	636	δ C ₆ C ₃₅ (29), δ PhI(15), δ C ₁₂ O ₁₆ (12)
625	18.22	5.69	-	-	δ PhII(44)
614	39.63	5.78	-	-	δ PhII(35), δ C ₃₁ O ₃₂ (14)
612	60.95	2.41	-	-	γ N ₁₀ H ₁₁ (73)
601	96.01	6.18	-	600	γ O ₃₇ H ₃₈ (50), γ ring(10)
597	34.60	9.87	596	-	γ C ₂₈ C ₃₁ (61)
578	6.03	5.27	572	578	δ C ₁₈ O ₁₉ (41), δ C ₃₁ O ₃₂ (18)
549	27.23	18.37	547	-	δ PhI(17), δ ring(16), δ C ₆ C ₃₅ (15)
516	18.76	0.89	535	-	δ ring(46), δ C ₃₅ O ₃₆ (13)
511	25.17	2.65	511	-	γ PhI(37), γ ring(22), γ C ₆ C ₃₅ (13)
498	13.14	5.76	-	500	γ C ₂₁ N ₂₀ (29), γ PhII(39), γ C ₂₈ C ₃₁ (13)
489	7.07	1.35	-	-	δ PhII(25), δ C ₂₈ C ₃₁ (45)
471	47.81	1.55	459	-	δ C ₃₅ O ₃₆ (39)
438	28.55	1.58	438	437	δ C ₁₃ O ₁₅ (16), δ N ₂₀ H ₃₉ (13), δ C ₁₂ O ₁₆ (11)
433	4.83	0.13	426	-	γ PhI(54)
415	13.12	5.03	-	-	δ C ₁₈ O ₁₉ (41), δ C ₁₃ O ₁₅ (10)

405	0.21	0.06	406	-	γ PhII(80)
394	22.32	2.29	-	379	δ C ₁₈ C ₁₄ (23), δ C ₁₂ O ₁₆ (17), δ C ₂₁ N ₂₀ (13)
368	8.65	4.57	-	347	δ C ₃₁ O ₃₂ (17), δ ring (28), δ PhII(12)
317	0.36	0.74	-	-	γ C ₁₄ C ₁₈ (13), γ PhI (13), γ ring(11)
308	1.65	0.04	-	-	γ ring(21), γ C ₂₈ C ₃₁ (11), γ PhII(11)
307	13.3	0.88	-	-	δ C ₁₈ O ₁₉ (18), δ C ₂₁ N ₂₀ (21)
297	0.74	6.20	-	286	δ C ₃₅ C ₆ (17), δ C ₆ O ₃₅ (14), δ PhI(18)
253	0.37	1.19	-	-	γ C ₁₄ C ₁₈ (49), δ PhII(25)
247	0.86	0.78	-	-	γ C ₁₈ C ₁₄ (19), δ PhI(12)
181	0.43	0.85	-	196	δ PhII(24), δ C ₆ C ₃₅ (10)
176	0.10	2.02	-	-	τ ring(41), γ O ₁₅ H ₁₇ (22)
158	1.90	0.19	-	-	τ ring(24), γ N ₁₀ H ₁₁ (21)
150	5.09	0.13	-	-	δ C ₂₈ C ₃₁ (14), δ C ₁₈ O ₁₉ (13)
142	0.29	0.34	-	-	τ ring(20), τ C ₁₄ C ₁₈ (20)
116	3.03	0.67	-	-	δ C ₆ C ₃₅ (35)
104	0.13	1.20	-	101	τ C ₁₄ C ₁₈ (36), τ ring(18), γ O ₁₅ H ₁₇ (21)
78	2.32	1.57	-	-	τ C ₁₈ N ₂₀ (15), τ ring(11), τ PhI(10)
75	0.00	0.49	-	-	τ C ₂₈ C ₃₁ (60)
57	1.71	1.37	-	-	τ ring (15), τ PhI(14), τ C ₆ C ₃₅ (57)
49	0.00	0.75	-	-	τ ring(33)
47	0.03	0.80	-	-	δ N ₂₀ H ₃₉ (34), δ C ₂₁ N ₂₀ (11)
27	0.69	1.35	-	-	τ N ₂₀ C ₂₁ (57)
16	0.00	0.84	-	-	τ C ₁₈ N ₂₀ (29), τ C ₁₄ C ₁₈ (21), τ ring(12)

Table 3

Second-order perturbation theory analysis of Fock matrix in NBO basis corresponding to the intramolecular bonds of the title compound.

Donor(i)	type	ED/e	Acceptor(j)	Type	ED/e	E(2) ^a	E(j)-E(i) ^b	F(ij) ^c
C ₁ -N ₆	σ	1.98582	C ₁ -C ₂	σ*	0.05017	0.89	1.36	0.031
-	π	1.73005)	C ₂ -N ₃	π*	0.32058	18.49	0.31	0.069
-	π	-	C ₄ -C ₅	π*	0.04365	20.70	0.33	0.075
C ₂ -N ₃	π	1.70809	C ₁ -N ₆	π*	0.38561	20.02	0.29	0.069
-	π	-	C ₄ -C ₅	π*	0.29757	22.45	0.32	0.075
C ₄ -C ₅	σ	1.98640	C ₁ -N ₆	σ*	0.03033	0.61	1.21	0.024
-	π	1.62140	C ₁ -N ₆	π*	0.38561	20.47	0.26	0.065
-	π	-	C ₂ -N ₃	π*	0.32058	19.14	0.27	0.065
-	π	-	C ₉ -O ₁₀	π*	0.28710	10.70	0.31	0.053
C ₁₂ -C ₁₃	σ	1.97164	N ₁₁ -C ₁₂	σ*	0.03414	0.87	1.06	0.027
-	π	1.63542	C ₁₄ -C ₁₇	π*	0.39086	22.68	0.27	0.070
-	π	-	C ₁₅ -C ₁₉	π*	0.34201	20.85	0.29	0.070
C ₁₄ -C ₁₇	σ	1.97706	N ₁₁ -C ₁₂	σ*	0.03414	4.21	1.08	0.060
-	π	1.72017	C ₁₂ -C ₁₃	π*	0.38599	18.51	0.30	0.068
-	π	-	C ₁₅ -C ₁₉	π*	0.34201	19.17	0.31	0.070
C ₁₅ -C ₁₉	π	1.63333	C ₁₂ -C ₁₃	π*	0.38599	22.77	0.27	0.070
-	π	-	C ₁₄ -C ₁₇	π*	0.39086	23.23	0.26	0.070
LPN ₃	σ	1.92158	C ₁ -C ₂	σ*	0.05017	11.01	0.82	0.085
LPN ₃	σ	-	C ₄ -C ₅	σ*	0.04365	10.63	0.84	0.085
LPN ₆	σ	1.89228	C ₁ -C ₂	σ*	0.05017	11.12	0.81	0.086
LPN ₆	σ	-	C ₄ -C ₅	σ*	0.04365	10.21	0.83	0.084
LPO ₁₀	π	-	C ₅ -C ₉	σ*	0.07420	18.84	0.62	0.098

LPO ₁₀	π	-	C ₉ -N ₁₁	σ^*	0.07354	22.46	0.65	0.109
LPN ₁₁	σ	-	C ₉ -O ₁₀	π^*	0.28710	50.74	0.29	0.109
LPN ₁₁	σ	-	C ₁₂ -C ₁₃	π^*	0.38599	31.00	0.31	0.088
LPCl ₂₇	n	1.91841	C ₁ -N ₆	π^*	0.38561	14.26	0.27	0.060

Table 4

NBO results showing the formation of Lewis and non-Lewis orbitals of title compound.

Bond(A-B)	ED/ea	EDA%	EDB%	NBO	s%	p%
σ C ₁ -C ₂	1.99140	50.76	49.24	0.7125(sp ^{1.40})C	41.67	58.33
-	-0.78221	-	-	+0.7017(sp ^{1.77})C	36.14	63.86
σ C ₁ -N ₆	1.98582	39.57	60.43	0.6290(sp ^{1.87})C	34.86	65.14
-	-0.98582	-	-	+0.7774(sp ^{1.75})N	36.41	63.59
π C ₁ -N ₆	1.73005	45.46	54.54	0.6742(sp ^{1.00})C	0.00	100.00
-	-0.36803	-	-	+0.7385(sp ^{1.00})N	0.00	100.00
σ C ₁ -Cl ₂₇	1.98115	43.96	56.04	0.6630(sp ^{3.28})C	23.38	76.62
-	-0.70944	-	-	+0.7486(sp ^{5.94})C	14.42	85.58
σ C ₂ -N ₃	1.98229	40.06	59.94	0.6329(sp ^{2.18})C	31.47	68.53
-	-0.34997	-	-	+0.7742(sp ^{1.90})N	34.49	65.51
π C ₂ -N ₃	1.70809	42.91	57.09	0.6551(sp ^{1.00})C	0.00	100.00
-	-0.87490	-	-	+0.7556(sp ^{1.00})N	0.00	100.00
σ N ₃ -C ₄	1.98489	59.97	40.03	0.7744(sp ^{1.90})N	34.45	65.55
-	-0.86687	-	-	+0.6327(sp ^{2.24})C	30.82	69.18
σ C ₄ -C ₅	1.98640	49.27	50.73	0.7019(sp ^{1.69})C	37.19	62.81
-	-0.76925	-	-	+0.7122(sp ^{1.70})C	37.09	62.91

$\pi_{C_4-C_5}$	1.62140	49.06	50.94	0.7004(sp ^{1.00})C	0.01	99.99
-	-0.31939	-	-	+0.7137(sp ^{99.99})C	0.01	99.99
$\sigma_{C_5-N_6}$	1.97150	39.88	60.12	0.6315(sp ^{2.28})C	30.46	69.54
-	-0.87076	-	-	+0.7754(sp ^{1.86})N	34.96	65.04
$\sigma_{C_5-C_9}$	1.96638	52.10	47.90	0.7218(sp ^{2.08})C	32.43	67.57
-	-0.69127	-	-	+0.6921(sp ^{1.91})C	34.35	65.65
$\sigma_{C_9-O_{10}}$	1.98952	34.60	65.40	0.5883(sp ^{2.13})C	31.90	68.10
-	-1.00167	-	-	+0.8087(sp ^{1.97})O	33.67	66.33
$\pi_{C_9-O_{10}}$	1.97656	32.17	67.83	0.5672(sp ^{55.54})C	1.77	98.23
-	-0.42140	-	-	+0.8236(sp ^{54.69})O	1.80	98.20
$\sigma_{C_9-N_{11}}$	1.98598	36.36	63.64	0.6030(sp ^{2.12})C	32.03	67.97
-	-0.85300	-	-	+0.7978(sp ^{1.78})N	35.92	64.08
$\sigma_{N_{11}-C_{12}}$	1.98280	63.01	36.99	0.7938(sp ^{1.69})N	37.19	62.81
-	-0.81409	-	-	+0.6082(sp ^{2.68})C	27.16	72.84
$\sigma_{C_{12}-C_{13}}$	1.97164	51.28	48.72	0.7161(sp ^{1.68})C	37.34	62.66
-	-0.70877	-	-	+0.6980(sp ^{1.96})C	33.79	66.21
$\pi_{C_{12}-C_{13}}$	1.63542	51.24	48.76	0.758(sp ^{1.00})C	0.00	100.00
-	-0.26987	-	-	+0.6983(sp ^{1.00})C	0.00	100.00
$\sigma_{C_{12}-C_{14}}$	1.96297	50.28	49.72	0.7091(sp ^{1.82})C	35.41	64.59
-	-0.71281	-	-	+0.7051(sp ^{1.83})C	35.35	64.65
$\sigma_{C_{13}-C_{15}}$	1.97541	50.06	49.94	0.7075(sp ^{1.80})C	35.73	64.27
-	-0.69942	-	-	+0.7067(sp ^{1.80})C	35.67	64.33
$\sigma_{C_{14}-C_{17}}$	1.97706	50.02	49.98	0.7072(sp ^{1.74})C	36.45	63.55
-	-0.73587	-	-	+0.7070(sp ^{1.53})C	39.45	60.55
$\pi_{C_{14}-C_{17}}$	1.72017	48.11	51.89	0.6936(sp ^{1.00})C	0.00	100.00
-	-0.28552	-	-	+0.7203(sp ^{1.00})C	0.00	100.00

$\sigma_{C_{15}-C_{19}}$	1.96170	49.31	50.69	0.7022(sp ^{1.77})C	36.11	63.89
-	-0.69504	-	-	+0.7120(sp ^{1.93})C	34.07	65.93
$\pi_{C_{15}-C_{19}}$	1.63333	49.99	50.01	0.7070(sp ^{1.00})C	0.00	100.00
-	-0.25852	-	-	+0.7072(sp ^{1.00})C	0.00	100.00
$\sigma_{C_{17}-C_{19}}$	1.97709	50.40	49.60	0.7100(sp ^{1.43})C	41.11	58.89
-	-0.72842	-	-	+0.7042(sp ^{1.94})C	34.01	65.99
$\sigma_{C_{17}-I_{26}}$	1.97175	53.77	46.23	0.7333(sp ^{4.06})C	19.78	80.22
-	-0.49972	-	-	+0.6799(sp ^{8.65})C	10.37	89.63
$\sigma_{C_{19}-C_{22}}$	1.97831	50.95	49.09	0.7138(sp ^{2.14})C	31.89	68.11
-	-0.63165	-	-	+0.7004(sp ^{2.35})C	29.84	70.16
n1N ₃	1.92158	-	-	Sp2.21	31.11	68.89
-	-0.38057	-	-	-	-	-
n1N ₆	1.89228	-	-	Sp2.49	28.68	71.32
-	-0.37174	-	-	-	-	-
n1O ₁₀	1.97545	-	-	Sp0.55	64.52	35.48
-	-0.70487	-	-	-	-	-
n2O ₁₀	1.87439	-	-	Sp99.99	0.06	99.94
-	-0.27662	-	-	-	-	-
n1N ₁₁	1.65763	-	-	Sp99.99	0.07	99.93
-	-0.29824	-	-	-	-	-
n1I ₂₆	1.99300	-	-	Sp0.12	89.54	10.46
-	-0.61887	-	-	-	-	-
n2I ₂₆	1.97743	-	-	Sp99.99	0.14	99.86
-	-0.27418	-	-	-	-	-
n3I ₂₆	1.95066	-	-	Sp0.17	0.00	100.00
-	-0.27235	-	-	-	-	-

n1Cl ₂₇	1.99197	-	-	Sp0.17	85.15	14.85
-	-0.94724			-	-	-
n2Cl ₂₇	1.97091	-	-	Sp99.99	0.44	99.56
-	-0.33659			-	-	-
n3Cl ₂₇	1.91841	-	-	Sp1.00	0.00	100.00
-	-0.33348			-	-	-

Table 5

Second-order perturbation theory analysis of Fock matrix in NBO basis corresponding to the intra molecular bonds of CPCHODQ6C

Donor(i)	type	ED/e	Acceptor(j)	Type	ED/e	E(2) ^a	E(j)-E(i) ^b	F(ij) ^c
C ₅ -C ₆	σ	0.98733	C ₃₅ -O ₃₆	σ^*	0.13399	1.25	1.20	0.049
-	π	0.82446	C ₃₅ -O ₃₆	π^*	0.13399	14.41	0.24	0.076
-	π	-	C ₁ -C ₂	π^*	0.12995	11.73	0.28	0.074
C ₁₃ -C ₁₄	σ	0.98754	C ₄ -C ₅	σ^*	0.01001	1.84	1.26	0.061
-	σ	-	C ₁₈ -N ₂₀	σ^*	0.02628	1.55	1.16	0.054
-	π	0.84525	C ₁₂ -O ₁₆	π^*	0.00515	16.45	0.26	0.084
-	π	-	C ₁₈ -O ₁₉	π^*	0.13952	16.22	0.25	0.082
LPC ₄	σ	0.54382	C ₅ -C ₆	π^*	0.15882	35.28	0.15	0.111
-	σ	-	C ₁₃ -C ₁₄	π^*	0.17309	37.81	0.13	0.106
LPN ₁₀	σ	0.81494	C ₁₂ -O ₁₆	π^*	0.18382	27.67	0.26	0.108
LPO ₁₅	σ	0.98597	C ₁₃ -C ₁₄	σ^*	0.01569	4.22	1.06	0.085
-	π	0.88385	C ₁₃ -C ₁₄	π^*	0.17309	22.49	0.32	0.110

LPO ₁₆	σ	0.98828	N ₁₀ -C ₁₂	σ^*	0.03861	0.94	1.04	0.040
-	π	-	N ₁₀ -C ₁₂	σ^*	0.03861	11.50	0.62	0.107
-	π	-	C ₁₂ -C ₁₄	σ^*	0.02821	8.07	0.69	0.095
LPO ₁₉	π	0.92775	C ₁₈ -N ₂₀	σ^*	0.02662	8.34	0.79	0.105
LPN ₂₀	π	-	C ₁₈ -O ₁₉	π^*	0.98887	28.99	0.23	0.104
LPO ₃₂	π	0.93175	C ₂₈ -C ₃₁	σ^*	0.98606	7.71	0.67	0.093
LPO ₃₂	π	-	C ₃₁ -O ₃₃	σ^*	0.99564	16.26	0.54	0.119
LPO ₃₃	σ	-	C ₃₁ -O ₃₂	π^*	0.99259	21.43	0.30	0.106
LPO ₃₆	π	0.98819	C ₃₅ -O ₃₇	σ^*	0.99554	16.30	0.54	0.119
LPO ₃₇	π	0.91664	C ₃₅ -O ₃₆	π^*	0.13399	21.44	0.31	0.105

Table 6

Polarizability values of CPCHODQ6C with halogen substitutions

	μ debye	$\alpha \times 10^{-23}$ esu	$\beta \times 10^{-30}$ esu	$\gamma \times 10^{-37}$ esu	MR = $1.333\pi\alpha N$
CPCHODQ6C	3.7723	3.835	15.827	-37.219	$25.210 \times \alpha$
7F	2.4881	3.852	14.266	-40.117	97.113
8F	3.3922	3.835	18.475	-38.524	96.684
9F	4.0094	3.844	15.433	-38.203	96.911
7Cl	2.2885	4.090	14.706	-43.982	96.684
8Cl	3.3286	4.014	19.209	-41.111	103.113
9Cl	4.2570	4.019	16.340	-40.007	101.323
7Br	2.6165	4.200	14.325	-46.681	105.886
8Br	3.4016	4.103	18.702	-42.842	103.441
9Br	4.3456	4.097	14.845	-41.671	103.289

Table 7.

Values of solubility parameters δ [MPa^{1/2}] for studied molecules and selected frequently used excipients

Molecules	δ [MPa ^{1/2}]
CPCHODQ6C	27.411
PVP	18.515
Maltose	28.564
Sorbitol	32.425

Table 8

PASS prediction for the activity spectrum of CPCHODQ6C compound. Pa represents probability to be active and Pi represents probability to be inactive.

Pa	Pi	Activity
0.858	0.015	Ubiquinol-cytochrome-c reductase inhibitor
0.855	0.012	Methylenetetrahydrofolate reductase (NADPH) inhibitor
0.823	0.020	Testosterone 17beta-dehydrogenase (NADP+) inhibitor
0.777	0.017	Taurine dehydrogenase inhibitor
0.731	0.004	5 Hydroxytryptamine release inhibitor
0.732	0.014	Glutathione thiolesterase inhibitor
0.709	0.016	NADPH-cytochrome-c2 reductase inhibitor
0.705	0.015	2-Dehydropantoate 2-reductase inhibitor
0.700	0.012	Pterin deaminase inhibitor
0.690	0.005	N-methylhydantoinase (ATP-hydrolysing) inhibitor
0.711	0.026	Glutamate-5-semialdehyde dehydrogenase inhibitor
0.688	0.007	Aminobutyraldehyde dehydrogenase inhibitor
0.687	0.012	Kidney function stimulant
0.668	0.016	Fatty-acyl-CoA synthase inhibitor
0.673	0.029	Fusarinine-C ornithinesterase inhibitor
0.656	0.015	L-glutamate oxidase inhibitor
0.656	0.023	UDP-N-acetylglucosamine 4-epimerase inhibitor
0.641	0.008	Erythropoiesis stimulant
0.653	0.021	2-Hydroxyquinoline 8-monooxygenase inhibitor
0.639	0.007	Histamine release inhibitor
0.659	0.028	Ribulose-phosphate 3-epimerase inhibitor
0.646	0.017	Insulysin inhibitor
0.653	0.029	Dehydro-L-gulonate decarboxylase inhibitor

Table 9

The binding affinity values of different poses of the compound predicted by Autodock Vina.

Mode	Affinity (kcal/mol)	Distance from best mode (Å)	
-	-	RMSD l.b.	RMSD u.b.
1	-9.1	0.000	0.000
2	-8.7	23.021	25.648
3	-8.6	21.625	24.204
4	-8.5	4.709	6.627
5	-8.5	22.282	24.626
6	-8.2	15.464	16.890
7	-8.0	17.626	19.186
8	-8.0	2.659	10.111
9	-7.8	22.017	24.050

Figures

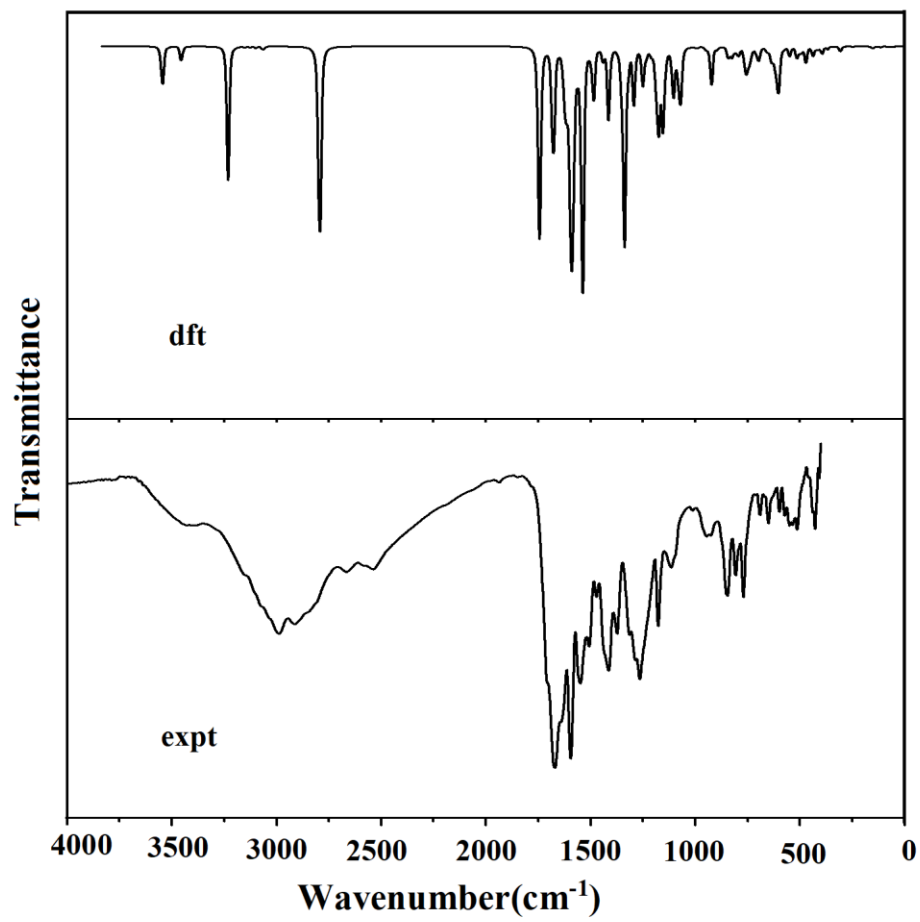


Fig. 1. FT-IR spectrum of CPCHODQ6C

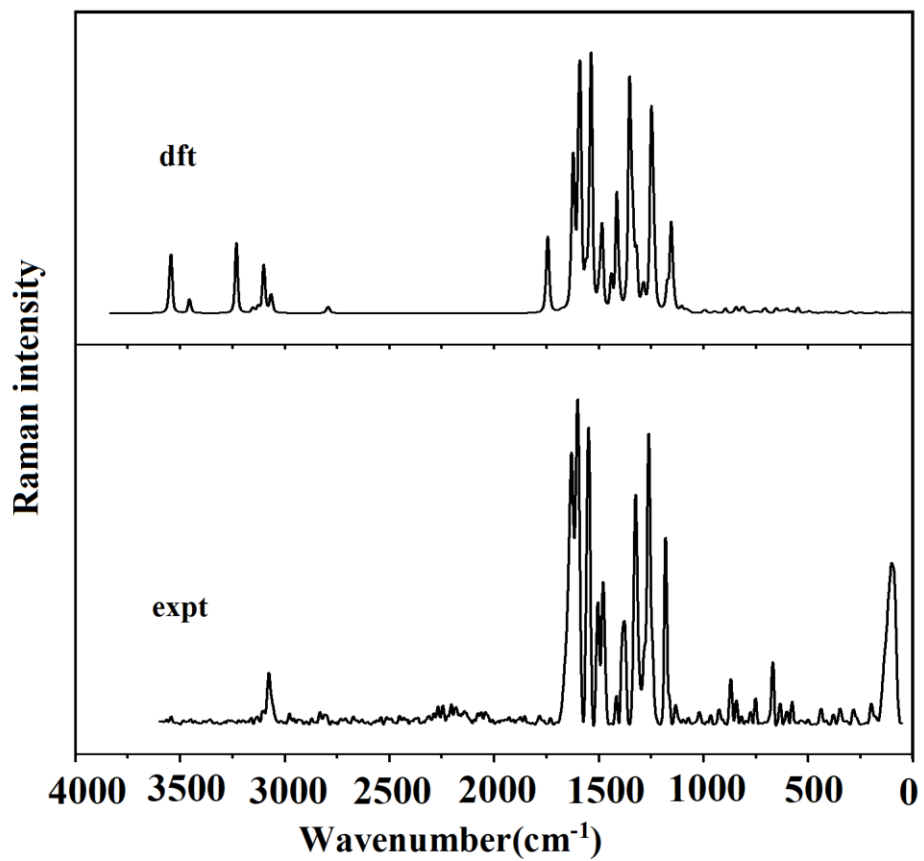


Fig. 2. FT-Raman spectrum of CPCHODQ6C

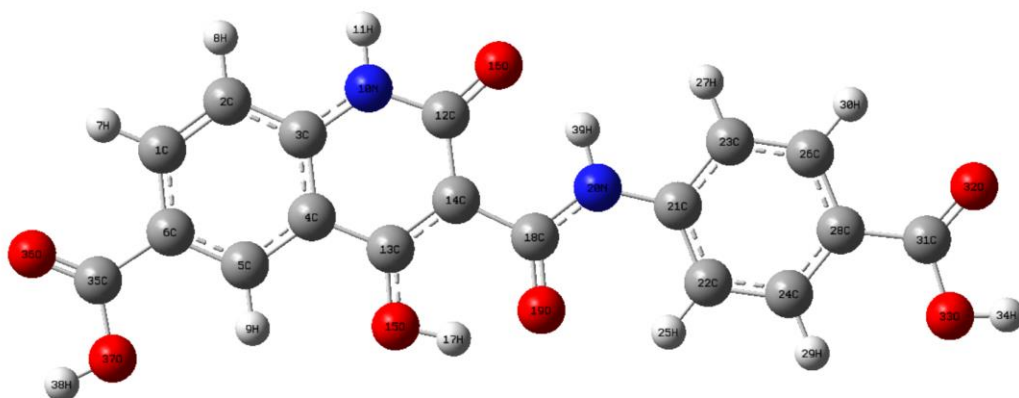


Fig. 3. Optimized geometry of CPCHODQ6C

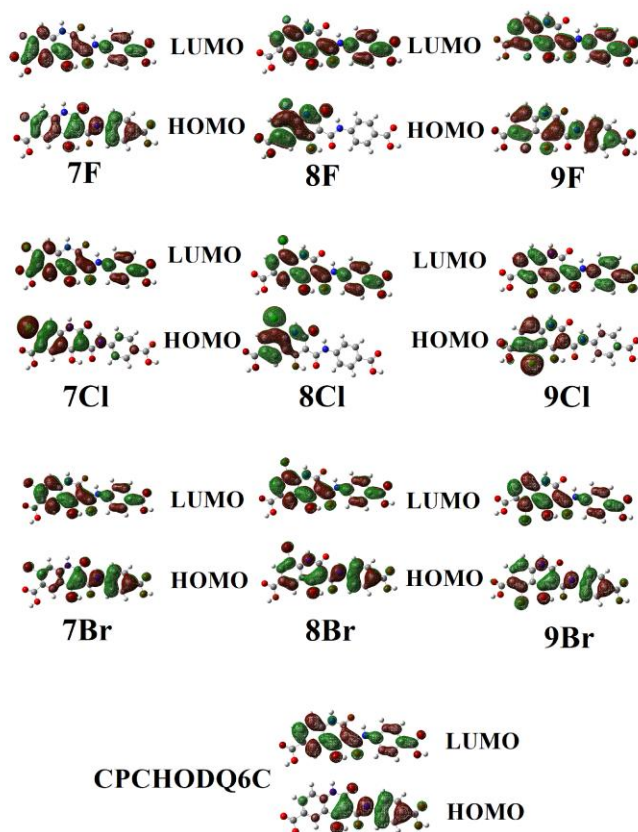


Fig. 4. HOMO-LUMO plots of CPCHODQ6C with halogen substitutions

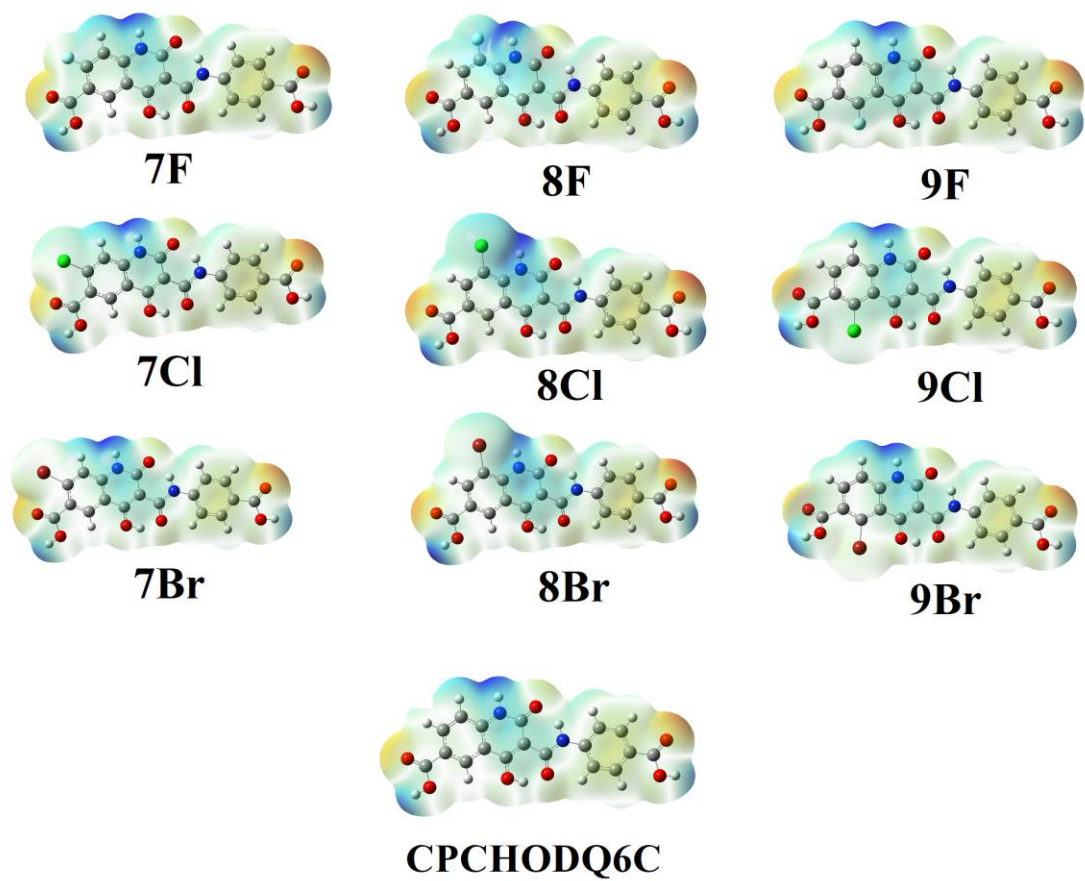
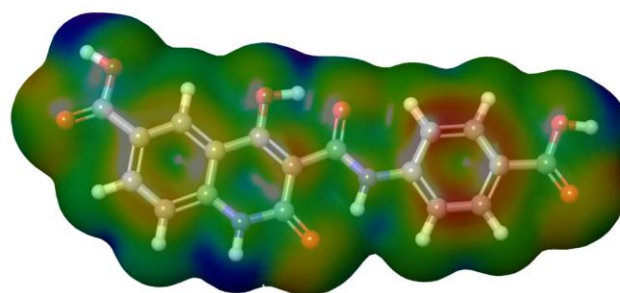


Fig. 5. MEP plots of CPCHODQ6C with halogen substitutions

ALIE



210.59 ALIE[Kcal/mol] 372.51



Fig. 6. ALIE surface of CPCHODQ6C

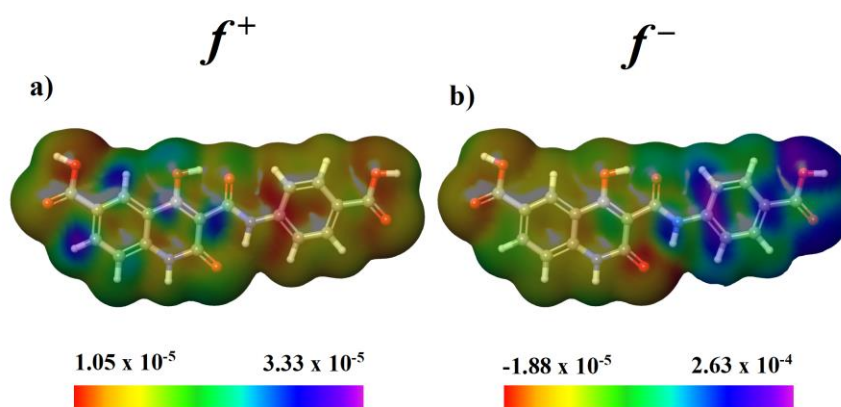


Fig. 7. Fukui functions a) f^+ and b) f^- of the CPCHODQ6C

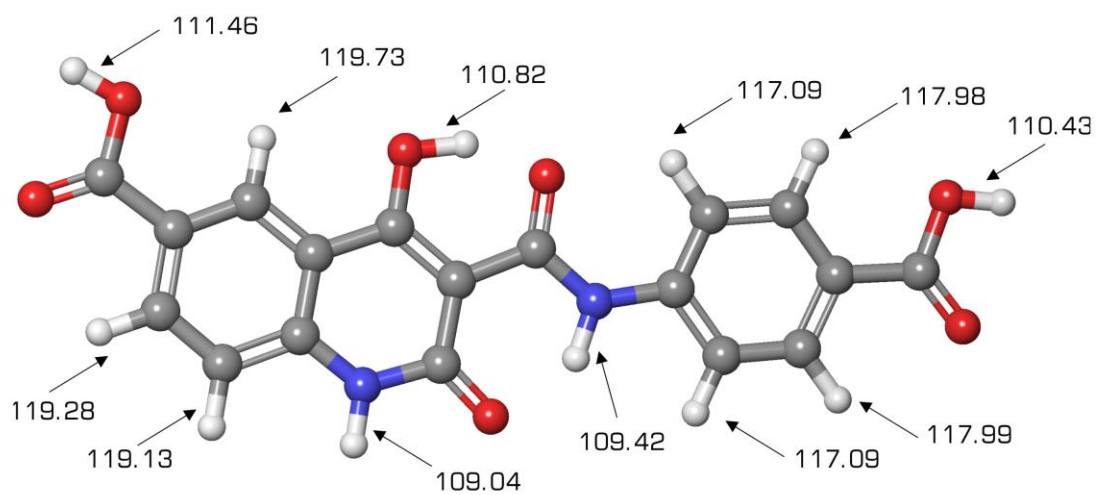


Fig. 8. BDEs of all single acyclic bonds of CPCHODQ6C

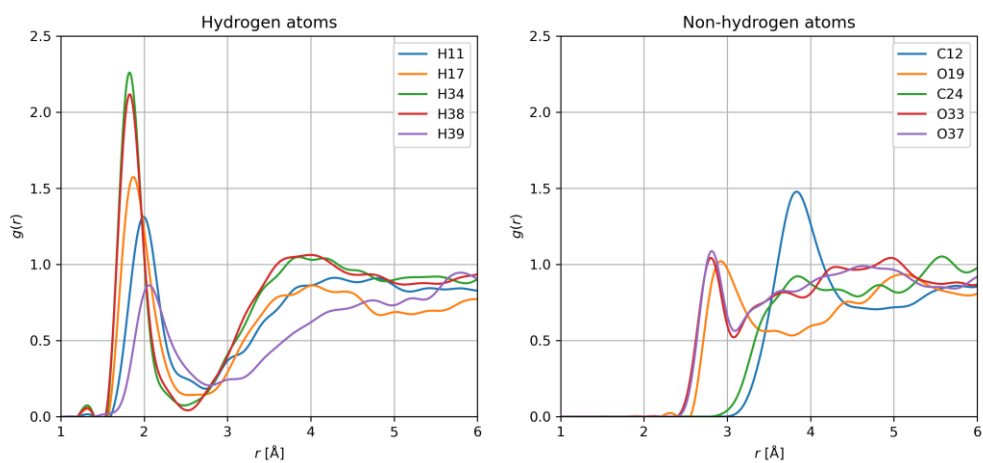


Fig. 9. RDFs of CPCHODQ6C atoms with significant interactions with water molecules

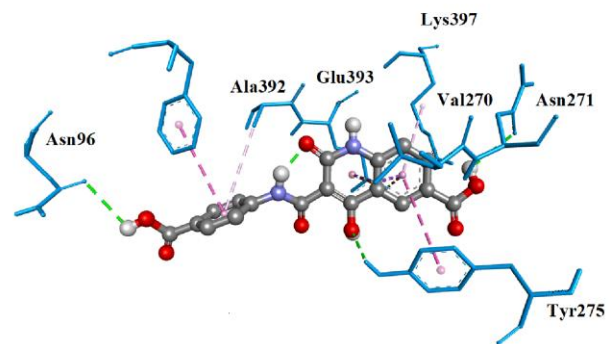


Fig. 10. Interactive plots of amino acids of the receptor with the ligand

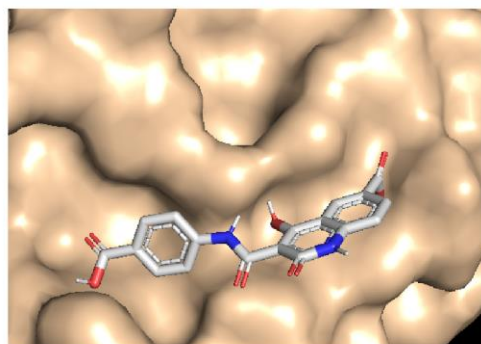


Fig. 11. The docked ligand of CPCHODQ6C at the active site of receptor



Fig. 12. The docked ligand embedded in the catalytic site of cytochrome BC1 complex